that his senses be employed in unique ways. Weight and space restrictions of a space vehicle are such that information flow to the man must be accomplished in the most efficient manner possible. This might require, for example, the use of olfactory cues for the presentation of discrete signals which may be widely spaced. Such signals might be employed to signify equipment component malfunction. Some equipment malfunctions may result in olfactory cues which do not occur by design. Olfactory signalling systems may be constructed of very small size with very low power requirements while at the same time they may encompass an appreciable number of discretely coded signals. Unpleasant odors derived from paint and other materials employed in the construction of a space vehicle, from equipment failure, or which are of the occupant's own production must be eliminated or controlled. Although there is usually fairly rapid and complete adaptation of the olfactory sense, the aversive effects of some odors may continue over a long period.

Gustatory Sense

The sense of taste may not play any direct role in man's performance in space flight but it will be of importance if he is to be kept well and happy on an extended mission. He must be provided with palatable food which is manageable in the zero G environment of outer space and which will not create unnecessary problems of waste disposal.

OTHER PROBLEMS

Time Perception

It has been speculated that in the absence of acceleration and the resulting lack of the requirement of continuous tension to maintain posture, the occupants of a space vehicle may require little or no sleep. This may grossly affect such things as the perception of the passage of time. The gross distortion of time perception may have severe effects, both practical and psychological, on an individual who has undergone extensive prior training at 1 G without time distortion. It may also render irrelevant work

done at the surface of the earth in a 1 G environment on the subject of sleep-rest cycles.

Sensory Deprivation

Some concern has been expressed over the implications of studies of sensory deprivation for space flight. Although there has been considerable variability in the results of these experiments, some of them indicate that in the absence of the usual pattern of sensory inputs, man may suffer serious psychological and perceptual disruptions.[22] Although his environment will be severely limited within the confines of a space vehicle, man in space will not be deprived of sensory inputs in the same sense that subjects of sensory deprivation experiments have been deprived, however. It will be surprising if the restricted environment of the space vehicle and the limitations on the variety of sensory experience do not have profound psychological effects on the members of space missions. It seems highly improbable that these effects can be predicted from sensory deprivation studies, however.

REFERENCES

1. Adams, C. C.: .*Space Flight*. McGraw-Hill; New York, 1958.
2. Baker, C. A.: *Man's Visual Capabilities in Space*. Proc. Seventh Annual East Coast Conference on Aeronautical and Navigational Electronics, October, 1960.
3. Boynton, R. M., Elsworth, C., and Palmer, R. M.: Laboratory studies pertaining to visual air reconnaissance. *WADC Tech. Rept. 53-304*, Part III. Wright-Patterson Air Force Base, Ohio, April, 1958.
4. Brown, J. L.: The bio-dynamics of launch and re-entry. *Mil. Med., 124*:775–781, 1959.
5. Brown, J. L.: Acceleration and motor performance. *Human Factors, 2*:175–185, 1960.
6. Brown, J. L.: Flash blindness. *Tech. Rept. Missile and Space Vehicle Dept.* General Electric Co., September, 1961.
7. Brown, J. L., editor: *Sensory and Perceptual Problems Related to Space Flight*. Washington, Nat. Acad. Sci.-Nat. Res. Council, Pub. No. 872, 1961.
8. Brown, J. L.: Orientation to the vertical during water immersion. *Aerospace Med., 32*:209–217, 1961.

9. Brown, J. L., and Burke, R. E.: The effect of positive acceleration on visual reaction time. *J. Aviat. Med.*, 29:48–58, 1958.
10. Brown, J. L., Ellis, W. H. B., Webb, M. G., and Gray, R. F.: *The Effect of Simulated Catapult Launching on Pilot Performance.* Rept. NADC Ma 5719, U. S. Naval Air Dev. Cen., Johnsville, Pa., December, 1957.
11. Brown, J. L., and Lechner, M.: Acceleration and human performance. *J. Aviat. Med.*, 27:32–49, 1956.
12. Brown, R. H.: "Empty-field" myopia and visibility of distant objects at high altitudes. *Am. J. Psychol.*, 70:376–385, 1957.
13. Clark, B., and Graybiel, A.: *Human Performance During Adaptation to Stress in the Pensacola Slow Rotation Room.* U. S. Naval School of Aviat. Med., Pensacola, Fla. Proj. MR 005.13-6001, Subtask 1, Rept. No. 2, May, 1960.
14. Cochran, L. B., Gard, P. W., and Norsworthy, M. E.: *Variations in Human G Tolerance to Positive Acceleration.* Rept. 001 059 02.10 U. S. Naval School of Aviat. Med., Pensacola, Fla. August, 1954.
15. Collins, C. C., Crosbie, R. J., and Gray, R. F.: *Pilot Performance and Tolerance Studies of Orbital Reentry Acceleration.* Letter Rept. TED ADC AE 1412. U. S. Naval Air Dev. Cen., Johnsville, Pa., September, 1958.
16. Cordes, F. C. Eclipse retinitis. *Am. J. Ophthal.*, 31:101, 1948.
17. Culver, J. F., and Newton, N. L.: *Early Ocular Effects of High-energy Proton and Alpha Radiation.* USAF Sch. Aviat. Med., Brooks AFB, Texas, 1961.
18. Duane, T. D.: Observations of the fundus oculi during blackout. *Arch. Ophthal.*, 51:343–355, 1954.
19. Duane, T. D., Beckman, E. L., Ziegler, J. E., and Hunter, H. N.: *Some Observations on Human Tolerance to Exposures of 15 Transverse G.* Rept. NADC Ma 5305. U. S. Naval Air Dev. Cen., Johnsville, Pa., July, 1953.
20. DuBridge, L. A.: *Introduction to Space.* New York, Columbia Univ. Press, 1960.
21. Duke-Elder, W. S.: *Textbook of Ophthalmology,* Vol. I. C. V. Mosby Co., 1942. pg. 815 ff.
22. Freedman, S. J.: Perceptual changes in sensory deprivation: Suggestions for a conative theory. *J. Nerv. Ment. Dis.*, 132:17–21, 1961.
22a. Geldard, F. A.: Adventures in tactile literacy. *Am. Psychologist*, 12:115–124, 1957.
23. Gernandt, R. E.: Vestibular mechanisms. Ch. XXII in *Neurophysiology* Section I, Vol. I of *Handbook of Physiology.* Am. Physiol. Soc., Washington, 849, 1959.

24. Graybiel, A., Clark, B., and Zariello, J. J.: Observations on human subjects living in a "slow rotation room" for periods of two days. *Arch. Neurol., 3*:55–73, 1960.
25. Haber, H.: Manned flight at the borders of space. *J. Am. Rocket Soc., 22*:3–269, 1952.
26. Hall, R. J., Brown, H. T., Payne, T. A., and Rogers, J. G.: *Detection Stereotopy.* Rep. SD 60-119, Hughes Aircraft Co., Fullerton, Calif., December, 1960.
27. Haviland, R. P.: A concept of space travel and operations. *Visual Problems of the Armed Forces.* Armed Forces–NRC Committee on Vision, March 30–31, 1961. Ed. by M. A. Whitcomb, pp. 37–48.
28. Ittleson, W. H.: .*Visual Space Perception.* New York, Springer, 1960.
29. Johnson, F. S.: The solar constant. *J. Meteorology, 11*:431, 1954.
30. Jones, E. R., and Hann, W. H.: Vision and the Mercury capsule. *Visual Problems of the Armed Forces.* Armed Forces–NRC Committee on Vision, March 30–31, 1961. Ed. by M. A. Whitcomb. pp. 49–65.
31. Joyce, W., and Mallett, F.: *Navigation Techniques and Displays for Interplanetary Space Flight.* Ohio State Univ. Found., Columbus, Ohio: December, 1959, Rep. No. 813.
32. Kilpatrick, F. P.: Two processes in perceptual learning. *J. Exper. Psychol., 47*:362–370, 1954.
33. Konecci, E. B., and Trapp, R.: Calculations of the radiobiologic risk factors in nuclear powered space vehicles. *Aerospace Med., 30*:487–506, 1959.
34. Lansberg, M. P.: The function of the vestibular sense and the construction of a satellite. *Aeromed. Acta, 4*:183–190, 1955.
35. Margaria, R., and Gualtierotti, T.: Body susceptibility to high accelerations and to zero gravity condition. *Advances in Aeronautical Sciences.* New York, Pergamon Press, 1961. pp. 1081–1103.
36. McDonald, T. C.: Changing concepts in aviation medicine. *J. Aviat. Med., 26*:463, 1955.
37. Mickelwait, A. B., Tomkins, E. H., and Park, R. A.: Interplanetary navigation. *Sc. Am., 202*:64–73, 1960.
38. Miller, J. W., and Ludvigh, E.: The perception of movement persistence in the Granzfeld. *J. Opt. Soc. Am., 51*:57–60, 1961.
39. Pirie, A.: Recovery from and protection against radiation damage to the lens. In *The Structure of the Eye.* Ed. by Smelser, G. K. Academic Press, 1961, New York and London.
40. Schaefer, H. J.: *Further Evaluation of Tissue Depth Doses in Proton Radiation Fields in Space.* Nav. School Aviat. Med., Pensacola, Fla., Proj. No. MR 005.13-1002, Subtask No. 1, Rept. No. 17, 1960.
41. Strughold, H.: The human eye in space. *Astronautica Acta, 5*, 1960.

42. Stumpe, A. R.: Health hazards of new aircraft and rocket propellents. *J. Aviat. Med.*, 29:650–659, 1958.
43. Swartz, W. F., Obermayer, R. W., and Muehler, F. A.: *Some Theoretical Limits of Man-periscope Visual Performance in an Orbital Reconnaissance Vehicle.* Baltimore, The Martin Co., 1959, Engrg. Rept. No. 10978.
44. Teuber, H. L., and Bender, M. B.: Neuroophthalmology: The oculomotor system. *Prog. Neurol. Psychiat.*, 6:148–178, 1951.
45. Toolin, R. B., and Stakutis, V. J.: Visual albedo and total solar illumination as a function of altitude. *Bull. Am. Meteorol. Soc.*, 39:543, 1959.
46. White, W. J.: *Variations in Absolute Visual Thresholds During Acceleration Stress.* WADC Technical Rept. 60-34, Wright-Patterson AFB, Ohio, April, 1960.
47. White, W. J.: Visual performance under gravitational stress. Ch. 11 in *Gravitational Stress in Aerospace Medicine*, ed. by Gauer and Zuidema. Boston, Little, Brown and Co., 1961.
48. White, W. J., and Jorve, W. R.: *The Effects of Gravitational Stress upon Visual Acuity.* WADC Technical Report 56-247, Wright-Patterson AFB, Ohio, November, 1958.
49. White, W. J., and Riley, M. B.: *The Effects of Positive Acceleration on the Relation Between Illumination and Instrument Reading.* WADC Tech. Rept. 58-332, Wright-Patterson AFB, Ohio, November, 1958.
50. Whiteside, T. C. D.: The Problem of Vision in Flight at High Altitude. London, Butterworth's Scientific Publications, 1957.
51. Woodworth, R. S.: *Experimental Psychology.* New York, Holt, 1938.

POSTMASTER: MERCHANDISE — FOURTH CLASS
This package may be opened for postal inspection if necessary. Postage for return guaranteed by sender.

Lawrence Dunkelman

Institute for Defense Analyses
Research and Engineering Support Division
1666 CONNECTICUT AVENUE, N.W., WASHINGTON 9, D.C.

to:

Sherman P. Vinograd, M.D.
Chief, Medical Science & Technology
Branch
Space Medicine Division
NASA Office of Manned Space Flight
Washington, D. C.

My new address & tel. no. for you & Al to note. Give him my regards

Lawrence Dunkelman

[redacted]

INSTITUTE FOR DEFENSE ANALYSES
Research and Engineering Support Division
400 Army Navy Drive Arlington, Va. 22202
558-1648 (Area Code 703)

28 October 1964

John A. Buesseler, M.D.
Professor and Chief of Opthamology
University of Missouri School of Medicine
Columbia, Missouri

Dear Dr. Buesseler:

You will recall that we had a brief discussion at the George Washington University on extraterrestrial solar illuminance and ultraviolet irradiance after your very interesting and informative lecture during the current short course on Engineering Aspects of Space Medicine. This letter is a follow-up of our discussion.

I am enclosing several reprints which may be of interest to you. The papers are listed on a separate page. In Paper A, page 367, we give a value of solar illuminance outside the atmosphere at 12,700 $\pm$ 400 lumens ft^{-2} (foot candles). Note also that in this paper values for spectral exponential attenuation coefficients of the total vertical atmosphere (above Mount Lemmon, near Tucson, Arizona, altitude 8,025 feet) are given in the table on page 363 and curve on page 364.

Papers B and C are included for general interest to show horizontal attenuation of ultraviolet light by the lower atmosphere, Paper D for atmospheric turbidity, and Paper E for day sky brightness measurements from a rocket. Papers F and G are typical of recent publications of the solar intensity distribution measurements made from rockets above the atmosphere. Finally, Papers H and I are included as examples of astronaut visual and photographic measurements of night glow, J for day ultraviolet earth albedo measurements from a rocket, and K and L as examples of ultraviolet detectors and instrumentation to permit an astronaut to see middle and far ultraviolet phenomena by means of an image converter.

With best wishes,

Lawrence Dunkelman

LD:bh

Enclosures - As Stated

cc: Sherman P. Vinograd, M.D.
Chief, Medical Science and Technology Br.
Space Medicine Division
NASA Office of Manned Space Flight
Washington, D. C.

ENCLOSURES

PAPER

A. Solar Spectral Irradiance and Vertical Atmospheric Attenuation in the Visible and Ultraviolet, by L. Dunkelman and R. Scolnik, J. Opt. Soc. Am., 49, 356-367 (1959).

B. Horizontal Attenuation of Ultraviolet Light by the Lower Atmosphere, by William A. Baum and Lawrence Dunkelman, J. Optc. Soc. Am., 45, 166-175 (1955).

C. Horizontal Attenuation of Ultraviolet and Visible Light by the Lower Atmosphere, by Lawrence Dunkelman, Naval Research Laboratory, Report No. 4031 (1952).

D. Atmospheric Turbidity and its Spectral Extinction, by F. Volz, Review Geofisica Pura E Applicata, 31, 119-123 (1955).

E. Day Sky Brightness to 220 KM, by Otto E. Berg, J. Geophys. Res 60, 271-277 (1955).

F. The Intensity Distribution in the Ultraviolet Solar Spectrum, by C. R. Detwiler, D. L. Garrett, J. D. Purcell and R. Tousey, Annales de Geo., 17, 9-17 (1961).

G. The Solar Spectrum From 2635 to 2085 A, by H. H. Malitson, J. D. Purcell, and R. Tousey, and C. E. Moore, Ap. J. 132, 746-766 (1960).

H. Visual Observations of Nightglow From Manned Aircraft, by M.S. Carpenter, J.A. O'Keefe, and L. Dunkelman, Science 138, 978-980 (1962).

I. Photographic Observations of the Airglow Layer, by F. C. Gillett, W. F. Hugh, and E. P. Ney, Geo. Res. 69, 2827-2834 (1964).

J. Middle Ultraviolet Day Radiance of the Atmosphere, by J. P. Hennes, W. B. Fowler, and L. Dunkelman, J. Geo. Res. 69, 2835-2840 (1964).

K. Middle Ultraviolet Photoelectric Detection Techniques, by Lawrence Dunkelman, John P. Hennes, and Walter B. Fowler, Proceedings of the Third International Space Science Symposium at Washington, April 30-May 9, 1962, published in Space Research III (1963).

L. Ultraviolet Photography and Spectroscopy Using A Spectrally Selective Image Converter, by Lawrence Dunkelman and John Hennes, presented at the ICO Conference on Photographic and Spectroscopic Optics, Tokyo and Kyoto, Japan, September 1-8, 1964, to be published in a Supplement to the Japanese J. Applied Physics, May 1965.

Solar Spectral Irradiance and Vertical Atmospheric Attenuation in the Visible and Ultraviolet

L. Dunkelman and R. Scolnik

Reprinted from Journal of the Optical Society of America, Vol. 49, No. 4, pp. 356–367, April, 1959

Reprinted from JOURNAL OF THE OPTICAL SOCIETY OF AMERICA, Vol. 49, No. 4, 356–367, April, 1959
Printed in U. S. A.

Solar Spectral Irradiance and Vertical Atmospheric Attenuation in the Visible and Ultraviolet

L. DUNKELMAN AND R. SCOLNIK
U. S. Naval Research Laboratory, Washington 25, D. C.
(Received August 21, 1958)

The solar spectral irradiance outside the earth's atmosphere was determined by Langley's method of extrapolation to zero air mass, from measurements taken on Mount Lemmon at an elevation of 8025 ft near Tucson, Arizona, during October, 1951. The spectrum was produced and the energy scanned by a Leiss quartz double-monochromator, detected by a 1P21 photomultiplier, amplified, and presented on a strip chart recorder. About twenty-five spectra were recorded from sunrise to noon, with band widths ranging from 10 A at 3030 A to 170 A at 7000 A. The equipment was calibrated frequently by recording the spectrum of a standard tungsten lamp. Compared with earlier work performed in this field, our results agree best with those of Pettit. There is good agreement with the direct measurements from a rocket obtained by Purcell and Tousey in 1954 and with the Sacramento Peak ultraviolet observations by Stair and Johnston in 1955. The change of solar intensity with air mass showed that the attenuation of the atmosphere above Mount Lemmon was approximately 15% higher than that for a Rayleigh atmosphere in the region 3400 A to 4650 A, where there is no absorption due to ozone. A discussion is included which emphasizes the importance of clear and constant atmospheres which are necessary to obtain accurate values of solar spectral irradiance outside the earth's atmosphere by the Langley method. The solar illuminance computed from spectral data was 12 700 lumens/ft².

I. INTRODUCTION

SINCE 1946 when rockets became available for scientific research, the Naval Research Laboratory has made a number of measurements of the relative spectral intensity distribution of sunlight outside the earth's atmosphere, with the radiation measured from the entire solar disk. The spectral range has been confined to regions below 4000 A. At the present writing, data have been published to 2200 A.[1,2]

During 1950–1951 intensive efforts were made to fix the absolute level of the rocket-derived solar spectral-irradiance curve by adjusting it to match the most reliable absolute data available from ground measurements. A search of the literature, however, showed a great variation in the solar data obtained by different experimenters. This was particularly true near 3300 A where the match with the rocket curve had to be made.

In Fig. 1, there are shown the better known measurements of solar radiation from the entire disk made prior to 1949. The Smithsonian data[3,4] are basically absolute, but are usually shown in relative units only. Pettit[5] normalized his relative spectral solar-irradiance curve against the Smithsonian curve at 4500 A, thereby placing his own on an absolute basis. Both the Smithsonian and Pettit's published curves* have been readjusted downward to make them conform to the new absolute energy values for the solar spectrum given by Smithsonian.[6] Stair[7] in 1947 made absolute measurements in the region 3000 A to 3300 A. The data of Hess,[8] Reiner,[9] and Götz and Schönmann[10] were published only as curves of relative intensity distribution. We have normalized these curves against Pettit's at 4725 A to make comparison simpler.

The large differences in intensity distribution below 4000 A are not likely to have been produced by solar variations. More probably they must be attributed to the many difficulties besetting the measurements themselves. Instrumental stray light is one of the more serious problems. In a single dispersing system, there may easily be sufficient stray light to produce an error in the ultraviolet end of the spectrum where the energy is low. Other errors may arise from the inclusion of sky radiation from the region surrounding the sun when a little haze is present. Still another problem is the accurate calibration of the equipment. This is usually performed with a standardized light source of established relative intensity distribution. Unless standard lamps used by different experimenters have been compared with one another, there will always be some uncertainty attached to the comparison of experimental data based upon them.

Probably the most treacherous step, however, is the

[1] Johnson, Purcell, Tousey, and Wilson, *Rocket Exploration of the Upper Atmosphere* (Pergamon Press, London, 1954), pp. 279–288.
[2] Wilson, Tousey, Purcell, Johnson, and Moore, Astrophys. J. 119, 590 (1954).
[3] Abbot, Fowle, and Aldrich, Smithsonian Misc. Collections 74, 7 (1923).
[4] C. G. Abbot, Gerlands Beitr. Geophys. 16, 4, 343 (1927).
[5] E. Pettit, Astrophys. J. 91, 159 (1940).
* Pettit plotted the Smithsonian irradiance curve for zero atmosphere in the region 4500 A to 7000 A, and determined the ratio of the area under the curve within a band of 100 A centered at 4500 A to the area under the whole curve. Using the Smithsonian value of 0.71 cal cm^{-2} min^{-1} for the interval 4500 A–7000 A, he calculated the irradiance at 4500 A to be 22.4 μw cm^{-2} A^{-1}. Repeating Pettit's calculations with the newer data in the 9th edition of the Smithsonian Physical Tables,[6] we found that the spectral irradiance at 4500 A should be 20.3 μw cm^{-2} A^{-1}.
[6] Smithsonian Physical Tables, Ninth Revised Edition (1954), Table No. 812.
[7] R. Stair, J. Research Nat. Bur. Standards 40, 9 (1948).
[8] P. Hess, "Untersuchungen über die spektrale energieverteilung im sonnenspektrum von 350 mμ bis 500 mμ," Inaugural-Dissertation, Universität Frankfurt a.M. (1938).
[9] H. Reiner, Gerlands Betr. Geophys. 55, 2, 234 (1939).
[10] F. W. P. Götz and E. Schönmann, Helv. Phys. Acta 21, 151 (1948).

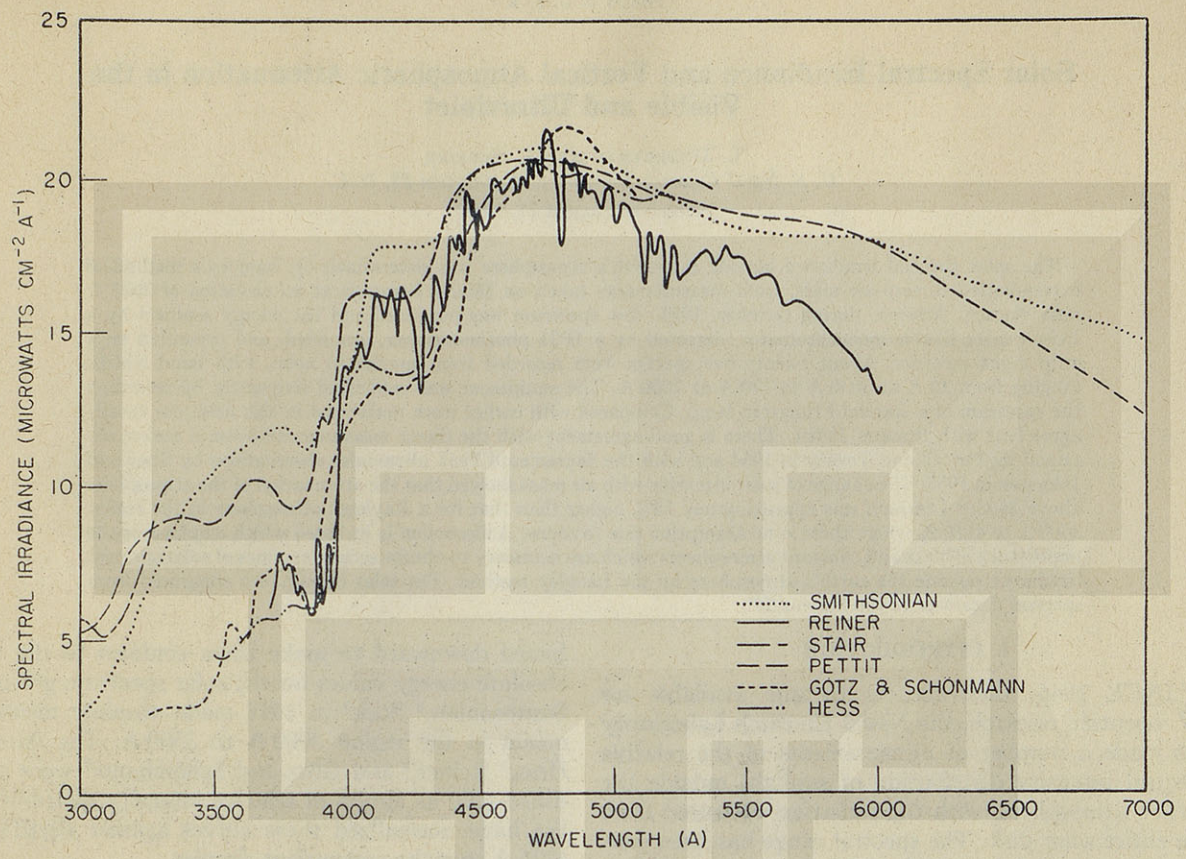

FIG. 1. Solar spectral irradiance curves outside earth's atmosphere obtained by various observers prior to 1949. The Smithsonian and Pettit curves are on an absolute scale. The curves of Reiner, Hess, and Götz and Schönmann are normalized to Pettit's curve at approximately 4700 A. Stair's curve is on an independent absolute scale.

extrapolation of the data measured on the ground to a level above the atmosphere. In the Langley method, measurements are made during all or part of a solar excursion between the horizon and the highest position attained by the sun during the day. The measured intensity, I, is related to the intensity outside the earth's atmosphere, I_0, by

$$I = I_0 e^{-\sigma m}, \tag{1}$$

where σ is the coefficient of attenuation, and m, usually referred to as the air mass, is the ratio of the path length through the atmosphere from the sun to the earth to the path length at vertical incidence. If the measured values of Log I are plotted against air mass, a straight line should result, and an extrapolation to zero atmosphere can be made. As will be emphasized later, only under ideal atmospheric conditions do the data measured over an entire day lie on a single straight line. Under nonideal conditions, if the measurements are collected over a small range of air mass values, the data may appear to fall on a straight line, but data over a wider range of air mass would have shown an actual departure. In such cases extrapolation to zero air mass leads to an erroneous solar intensity.

In an attempt to resolve the differences among the early investigators, and thereby to fix the absolute level of our own rocket results, we undertook, in 1951, to determine the relative solar spectral intensity extrapolated to zero atmosphere, taking advantage of the most recent advances in detecting and recording equipment, and selecting a site where measurements could be made under most ideal atmospheric conditions.

II. THE SITE

A basic requirement for applying the Langley method accurately is that the atmosphere be homogeneous over the portions of the sky covered by the sun-to-instrument path during the course of an entire morning, or afternoon, or both. For this condition to exist, the sky must be stable with passing time, and uniform over a wide geographical region. These requirements are most likely to be met when the sky is very clear, that is, free from clouds, haze, and dust. A high altitude is important, not only for the gain in energy reaching the instrument, but also because the less of the earth's atmosphere that remains overhead, the shorter and the more accurate will be the extrapolation to zero atmosphere. The same reasoning suggests a season and latitude when the sun will reach a high altitude at noon.

Mount Lemmon, in southern Arizona, was selected

as the most promising site within the United States from the points of view of atmospheric clarity and stability. Reaching an altitude of 9180 ft, it is the highest peak in the Santa Catalina Mountain Range in the Coronado National Forest. The observing station was located on a huge flat-topped rock, altitude 8015 ft, jutting out from the top of the headwall of Upper Sabino Canyon. To the east, the view of the sun was unobstructed from about 15 min after sunrise, while to the west, the view was open until 30 min of sunset. To the south, the rock overlooked timbered Sabino Canyon immediately below, while in the distance lay the desert east of Tucson. About 100 yards to the north and separated by a pine grove lay the modern, then rarely traveled, Hitchcock Memorial Highway.

The abrupt 5600-ft rise of the terrain from the desert floor to the observatory rock, the wooded nature of the surroundings, and a prevailing north breeze ensured that the instrumentation was well above the level of transient dust and smoke. The winds, the temperatures, and the altitude were moderate enough to cause neither personal discomfort nor instrumentation difficulties. The humidity was always extremely low. The mountain was easily accessible and electric power was available. There were comfortable living quarters within two miles at the privately owned Summerhaven tract.

Contrary to expectation the sky above Mount Lemmon was found to be unsuitable for accurate solar measurements during most of the period September 20 to October 17, 1951 spent on the mountain. During the first ten days, only calibration checks and test measurements were made, for clouds overhead and smoke from forest fires in California made the sky totally unsuitable.

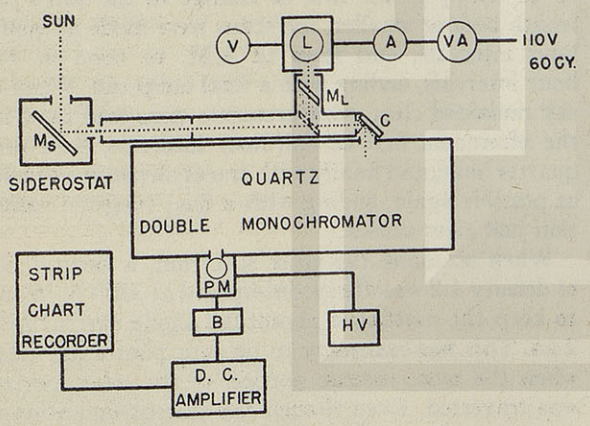

FIG. 2. Block diagram of the apparatus. Sunlight was introduced into the Leiss double monochromator from the magnesium carbonate block C. The block was illuminated either by sunlight, through the siderostat, or by the tungsten-in-quartz standard lamp L by interposition of mirror M_L. The lamp current and voltage were monitored continuously by means of voltmeter V and ammeter A and adjusted whenever necessary by variac VA. The 1P21 multiplier phototube detector was operated at a constant 600 v obtained from the regulated high-voltage power supply HV. The phototube current was amplified by the chopper amplifier and presented on the strip chart potentiometer recorder. The dark current was subtracted by means of the bucking box B.

At last, aided by the only day of rain encountered on the entire trip, the atmosphere cleared; and on October 4 we were able to make a full day's measurements with the clear stable sky required. Following this day, although the sky often seemed at first glance to be quite clear, careful examination showed faint wispy sky discontinuities which could not be described as true clouds, but which appeared and disappeared during the course of the day. Subsequent examination of the data confirmed our suspicions that the skies on these days were not sufficiently stable and uniform to permit accurate extrapolation to zero atmosphere.

In this paper we are reporting the results of the October 4 observations as the best data obtained. There are presented also data and curves showing how the accuracy of the measurements deteriorated on days when the sky appeared to be clear, but the atmospheric attenuation was not actually constant. These data may give some insight into the lack of agreement among the results of the many prior investigators.

III. APPARATUS

The equipment used for the solar measurements, shown in block form in Fig. 2, comprised basically a double monochromator that could be illuminated either by the sun through a siderostat, or by a standardized comparison lamp. Energy emerging from the exit slit was measured with a 1P21 multiplier phototube whose output was amplified and directed into a strip chart potentiometer recorder. The monochromator made by Carl Leiss was selected because of its compact and portable nature. Stray light was minimized through double-dispersion. The prisms were of quartz, and the radiation was collimated and focused by means of aluminized mirrors. Exit and entrance slits were maintained at 0.25 mm and center slit at 0.5 mm, resulting in a band pass that ranged from 10 A at 3030 A to 170 A at 7000 A. The monochromator was converted to automatic scanning and recording by coupling a motor drive to the wavelength-change drum. The instrument was installed in a light-tight box thermostatted to maintain a temperature of 85°F, which was the maximum reached during the heat of the day.

Sunlight was introduced into the instrument by means of a siderostat. This consisted of a mirror, M_s, which was rotated with a synchronous motor drive about an axis coinciding with the axis of rotation of the earth. With the siderostat, the angle of incidence on the mirror remained constant all day, thus obviating corrections for change of reflectance with angle of incidence.

After reflection from M_s, the sunlight was incident on a magnesium carbonate block placed in front of the monochromator entrance slit. The diffuse reflector served two functions: it eliminated the slight polarization arising at mirror M_s; and it caused the monochromator optical system to be filled at all times. If the

sunlight were not depolarized, an error would be introduced because the transmittance of the monochromator is slightly polarization dependent. Thus as mirror M_s rotated, the plane of polarization would have been changing continuously relative to the monochromator. The importance of keeping the optical system filled lay in the fact that the transmittance of the prisms was not constant across the aperture. Therefore, had the system been used in an unfilled condition, it would have been necessary to make sure that both the sunlight and the light from the calibrating lamp always passed through the same part of the optical system.

A system of baffles restricted the acceptance angle at the carbonate block to a cone of one degree diameter centered on the sun. This minimized the radiation accepted from the sky surrounding the sun. When the sky is hazy and an aureole is present, considerable light comes from the sky close to the sun. Inclusion of sky light may account for some of the discrepancies in the literature. In the Mount Lemmon work the sky contribution is negligible, because of the small acceptance angle used, and because no observations were made when the sky near the sun was appreciably hazy.

Since the measurements of solar radiation consisted of direct comparisons with radiation from a tungsten-in-quartz lamp,[11] it was necessary that both light beams be introduced under identical conditions. This was accomplished by reflecting the lamp radiation to the carbonate block by interposing the mirror M_L. The beams from the sun and from the lamp were of about the same angular subtense, and were incident on the block at the same angle. Mirrors M_s and M_L were front surfaced, aluminized together, and handled identically thereafter.

The tungsten reference lamp was calibrated by two completely independent procedures. The National Bureau of Standards determined the current at which to operate the lamp for a true temperature of 2805°K which corresponds to a color temperature of 2854°K. They also furnished a set of emissivity values based upon measurements of Hamaker[12] in the visible and the infrared, of Worthing[13] in the visible, and of Hoffmann and Willenberg[14] in the ultraviolet. In 1954, Devos[15] confirmed the emissivity values to 1% between 7000 A and 4000 A. Below 4000 A, Devos' values are lower, the difference being approximately 2% at 3400 A and reaching nearly 5% at 3100 A. This is well within our experimental error. From the emissivity values and the 2805°K blackbody distribution, the intensity distribution of the lamp radiation was calculated. A second calibration was performed at the Naval Research Laboratory with the assistance of Packer and Lock[16] using equipment they had assembled to measure the spectral radiance of the carbon arc. They used a quartz double monochromator of known spectral transmittance, and a phototube whose absolute spectral response had been determined by comparison with a thermocouple. The two sets of calibration results were in agreement within 5%.

[11] R. Stair and W. O. Smith, J. Research Natl. Bur. Standards **30**, 449 (1943).
[12] H. C. Hamaker, Thesis Utrecht (1934).
[13] A. G. Worthing, Phys. Rev. **10**, 377 (1917); Phys. Rev. **25**, 588 (1925); Z. Physik **22**, 9 (1924).
[14] F. Hoffmann and H. Willenberg, Phys. Z. **35**, 1, 713 (1934).
[15] J. C. Devos, Physica **20**, 690 (1954).

IV. PROCEDURE

A day's work began at a predawn hour when tarpaulins were removed and electric blankets were taken away, or not, according to the early morning temperature. The electronic instruments had been prewarmed to stable operation by use of a clock relay. The siderostat was capped, and the photomultiplier dark current balanced out by means of a microcurrent bucking circuit. The reference lamp was brought to the proper operating condition and a spectral traverse was made from 3000 A to 7000 A. By the time this was completed, the sun had cleared the trees to the east, and the day's first solar spectral trace could be started. The lamp mirror was withdrawn from the baffle allowing sunlight to enter the monochromator, the multiplier dark current was checked for zero balance, and the solar spectrum was recorded. At the end of the first scan, the wavelength drum was quickly returned by hand to the starting point, at 3000 A, and a new trace was begun immediately. All scans were made continuously in the direction of increasing wavelength.

Until about 10 A.M. spectral scans were made in rapid succession, with a lamp calibration interposed approximately every hour. A scan required 5 min, the return to starting point a matter of seconds. From 10 to 11 A.M., as the rate of change of the sun's path length became smaller, the scans were made at quarter hour intervals, and from 11 A.M. to noon at half-hour intervals, ending with a final lamp run. When the sky remained clear, measurements were continued into the afternoon, first at half-hour intervals, then every quarter hour, and finally with traces obtained as rapidly as possible again, ending with a final tungsten calibration just after sunset.

When scanning the solar spectrum, a neutral filter of density 1.2 was always interposed at 3800 A, in order to keep the multiplier phototube anode current below 2 μa. This was necessary to prevent phototube fatigue when the more intense portion of the solar spectrum was traversed. Even though the current limitation did not require it, the filter was also introduced at 3800 A for the reference lamp scans in order that optical conditions be maintained identical to those of the solar radiation measurements.

From 11:45 A.M. to 12:45 P.M. the air mass changed from 1.26 to 1.25 and back to 1.26, a negligible variation. Therefore, the noon hour was used for determining instrument stability and signal reproducibility

[16] D. M. Packer and C. Lock, J. Opt. Soc. Am. **42**, 879 (1952).

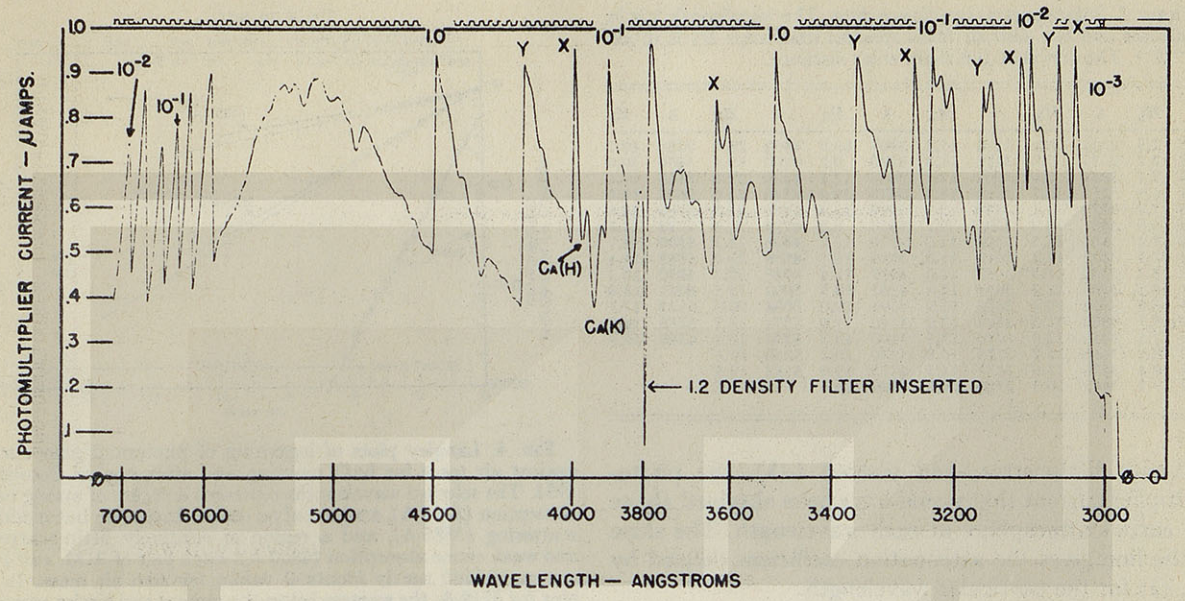

FIG. 3. A solar trace made at noon on the strip chart recorder. An amplifier recorder zero shown by 0 was recorded before each run Another zero shown by the 0 with solidus was recorded just before a run was begun and when the amplifier was set at the highest sensitivity and the sunlight blocked momentarily to insure that the dark current was entirely subtracted. Timing marks along the top were used for wavelength registration. Typical of solar features are the calcium H and K absorptions. The sharp spikes (10^{-n}, X, Y) are sensitivity range changes, not solar features.

and for checking the constancy of the sky. For example, the solar intensity at a single wavelength was recorded continuously for about 20 min to detect any variation in output or any sign of instability. On several days control voltages and temperatures were deliberately varied during the period of constant air mass to determine the magnitude of the effects of instrumental instability on the solar measurements. The precision estimate for the solar spectrum is based in part on this.

The noon hour was an ideal time for checking the monochromator for scattered and stray light. To do this the monochromator was set at 2850 A where no solar energy could possibly penetrate the earth's atmosphere. When the siderostat mirror was alternately capped and uncapped, the photocurrent change could be only that caused by radiation scattered within the monochromator. This was found to be less than 10^{-5} μa, an entirely negligible amount.

V. THE DATA

It cannot be over-emphasized that in order to obtain data valid for extrapolation to zero atmosphere, ideal sky conditions must prevail for the duration of a complete set of solar traces: i.e., from sunrise to noon, or from noon to sunset. In four weeks at Mount Lemmon, only three days were sufficiently clear and stable so that both morning and afternoon scans appeared worth analyzing. Three other days were satisfactory for the morning scan only. On the remaining days, sky conditions proved entirely unsatisfactory.

On October 4, 1951, the day of the nearest approach to the ideal stable sky, 26 traces of the solar spectrum and three of the tungsten standard lamp were recorded from noon to sunset. Figure 3 is a reproduction of a solar trace made at noon. The range change discontinuities in the solar curve are not to be confused with real spectral features. The actual full scale current value in microamperes is given at the point of each decade range change, while intermediate range changes are shown by X and Y, representing factors of 2 and 5, respectively.

The reduction of the traces was carried out at nearly 100 wavelengths between 3030 A and 6900 A. The wavelengths were those of distinct spectral features: maxima, minima, and points of inflection. All features were marked on each of the 26 traces, and the photocurrents corresponding to each of the selected wavelengths were tabulated. Next, for one wavelength at a time through the 26 traces, the log of the photocurrent was plotted against the air mass. The curves for 4850 A, 3585 A, and 3118 A, shown in Fig. 4, are typical and were selected as representative of regions of widely different character. For solar zenith angles from 0 to 75°, the air mass values are the secants of the angles. Beyond 75°, Bemporad's modifications[17] correcting for the curvature of the atmosphere and refraction were used.

Because of the clear, homogeneous, and constant atmospheric conditions on this day, the straight line relation held extremely well, even to air masses greater than ten, as can be seen from Fig. 4. This was true for all the wavelengths selected. Under these conditions, the extrapolation to zero atmosphere could be carried

[17] See reference 6, Table No. 811.

TABLE I. Solar spectral irradiance data. The wavelength λ is in angstroms and the zero air mass spectral irradiance H_λ is in $\mu w\ cm^{-2}\ A^{-1}$. The sun is at the mean solar distance.

λ	H_λ	λ	H_λ	λ	H_λ	λ	H_λ	λ	H_λ	λ	H_λ
3032	7.3	3221	8.1	3456	11.2	3807	13.5	4380	20.1	5380	19.7
3052	7.7	3225	7.5	3470	11.3	3830	9.2	4390	19.4	5450	20.0
3056	7.1	3242	8.9	3508	12.7	3848	12.1	4439	22.0	5525	19.4
3078	6.9	3255	12.7	3522	11.3	3870	10.4	4546	22.0	5604	19.0
3086	7.3	3279	11.1	3550	13.1	3908	13.4	4640	21.4	5700	18.8
3088	6.5	3301	13.2	3585	9.2	3933	8.6	4720	21.9	5758	18.7
3116	8.4	3308	11.5	3600	13.0	3950	12.2	4808	21.5	5800	18.7
3118	7.9	3322	11.3	3610	11.0	3968	10.1	4850	20.3	5842	18.4
3141	8.3	3330	11.3	3637	12.0	4019	19.4	4948	20.7	5980	18.2
3152	8.3	3335	11.2	3668	14.4	4062	18.5	5002	19.5	6021	18.0
3158	6.8	3368	10.4	3683	13.9	4094	20.0	5088	20.0	6122	17.1
3168	9.7	3380	11.3	3698	13.0	4140	19.6	5174	18.7	6280	16.6
3182	7.5	3410	12.3	3716	13.5	4190	18.2	5230	19.4	6500	15.9
3192	8.1	3414	11.7	3740	10.9	4220	20.2	5260	19.1		
3204	9.4	3430	11.9	3752	11.5	4272	19.0	5312	19.5		
3212	7.2	3442	10.3	3780	14.5	4300	16.1				

out with little error, and yielded $i_0(\lambda)$, the photomultiplier current that would have been obtained above the earth's atmosphere at each wavelength. The slope of the line gives the attenuation coefficient defined by Eq. (1) for the particular wavelength.

The current values $i_0(\lambda)$ were converted to relative values of solar spectral irradiance outside the atmosphere, $H_s(\lambda)$, by means of the traces made with the standard lamp. The several traces were found to be nearly identical, therefore, the average trace could be used. The relation is

$$H_s(\lambda)=i_0(\lambda)H_A(\lambda)/i_A(\lambda), \qquad (2)$$

where $H_A(\lambda)$ is the spectral irradiance on the magnesium carbonate block at wavelength λ produced by the standard lamp, and $i_A(\lambda)$ is the corresponding photomultiplier current as read from the average trace.

The relative values of $H_s(\lambda)$ are considered to be accurate to ±3%, except at the extremes of the wavelength range covered, where the error may be as high as ±6%. The chief reason for the increased error near the short wavelength limit is the feebleness of the photomultiplier current resulting from the low level of irradiation from the standard tungsten lamp. Near the long wavelength limit the increase in error is caused by the low sensitivity of the photomultiplier.

The original objective of the Mount Lemmon experiment was to obtain the solar intensity distribution on a relative scale only, and this is all that is intended by Eq. (2). However, an absolute calibration was obtained by measuring with a MacBeth Illuminometer the illuminance produced at the magnesium carbonate block by the tungsten standard lamp. This was compared with the illuminance computed from the relative spectral irradiance curve for the lamp, the conversion factor, 680 lu/w, and the CIE. Standard luminosity curve. The error in this process was judged to be ±10%. Later, Johnson,[18] from a study of the Smithsonian work on the solar constant, the intensity distribution curve obtained from rockets, and the present Mount Lemmon results, concluded that our original scale should be raised by 9%. The data presented here are on the absolute scale arrived at by Johnson.

[18] F. S. Johnson, J. Meteorol. **11**, 431 (1954).

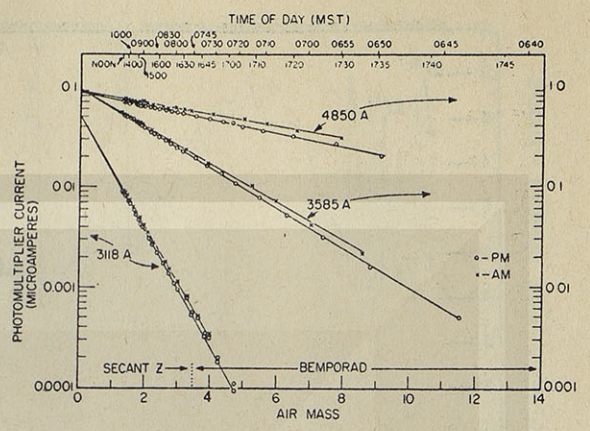

FIG. 4. Langley plots of logarithm of photomultiplier current against air mass for both morning and afternoon of October 4, 1951. The selected wavelengths represent a region of strong ozone absorption (3118 A), a region of no ozone absorption but moderate scattering (3585 A), and a region of relatively little scattering and weak ozone absorption (4850 A). Each pair of A.M. and P.M. curves yielded nearly identical values for zero air mass. In the plot for 3118 A, the squares below the crosses and circles represent the values obtained after correcting for the curvature of the ozonosphere.

VI. SOLAR IRRADIANCE

The final values of the solar spectral irradiance for zero atmosphere, with the sun at the mean solar distance, are given in Table I for the wavelengths of all the identifiable features of the records obtained at Mount Lemmon. These data to 4000 A are plotted as the solid curve in Fig. 5 which reveals all the Fraunhofer absorption detail that could be obtained from the measurements in this wavelength region. This may be compared with the two other recent curves shown. One was obtained by Purcell and Tousey[19] from the analysis of a solar spectrum photographed from a rocket at 104 km altitude on February 22, 1954. In this work the absolute energy scale was set by adjustment to the Mount Lemmon curve at 3600 A. The other curve is the result of the work of Stair and Johnston[20] carried out at Sacramento Peak in 1955. These data are to be preferred over the similar earlier work of Stair[21] in 1951 and of Stair, Johnston, and Bagg[22] in 1953. In 1955 the entire monochromator was automatically directed at the sun, thus avoiding the necessity of making a correction for polarization introduced by the siderostat used in the earlier work. The instrument used in 1955 was a Leiss double monochromator similar to that used at Mount Lemmon.

It may be seen that all three curves of Fig. 5 are in

[19] Purcell and Tousey (private communications).
[20] R. Stair and R. G. Johnston, J. Research Natl. Bur. Standards **57**, 205 (1956).
[21] R. Stair, J. Research Natl. Bur. Standards **49**, 227 (1952).
[22] Stair, Johnston, and Bagg, J. Research Natl. Bur. Standards **53**, 113 (1954).

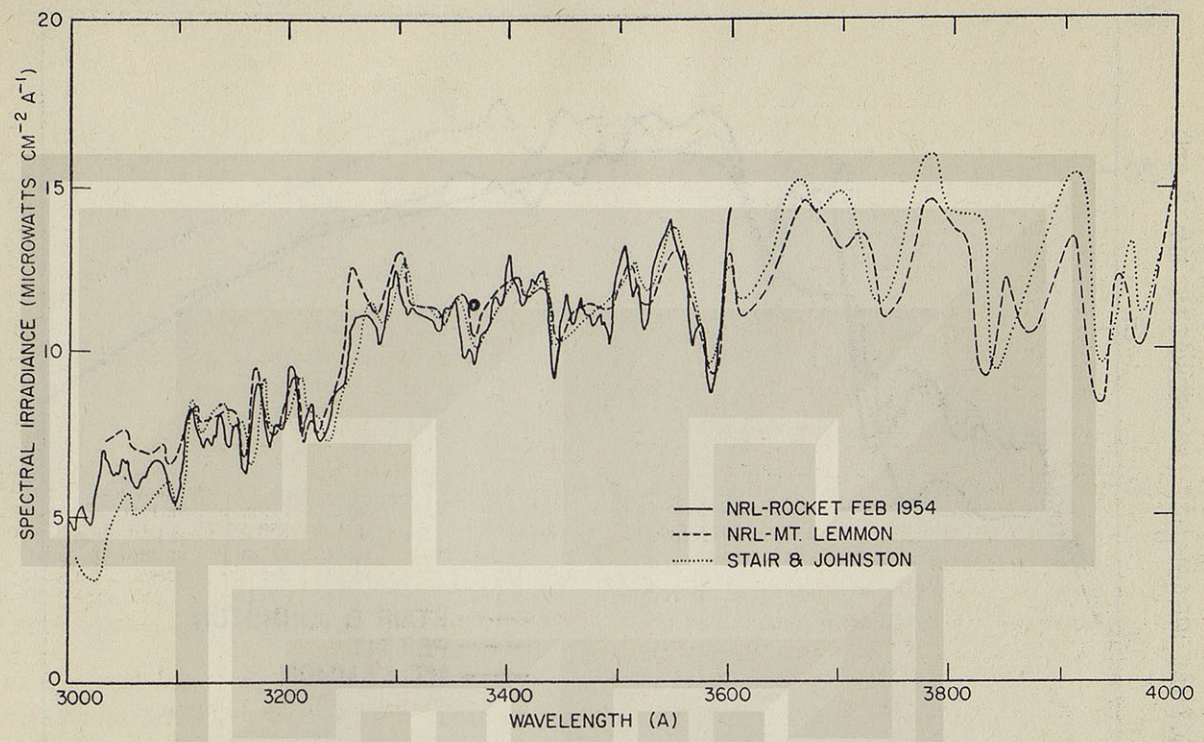

FIG. 5. A comparison of the solar spectral irradiance curves obtained by Stair and Johnston at Sacramento Peak, by Purcell and Tousey from a rocket at 104-km altitude, and by the authors at Mount Lemmon. The Mount Lemmon and the Stair and Johnston curves are plotted each according to its own absolute scale. The rocket curve, which begins at 3600 A was determined in relative units, and is plotted to give the best fit.

good agreement over this wavelength range. The variation below 3100 A is not unexpected because of the reduced energy available at the ground. Here the rocket curve, which actually extended to still shorter wavelengths, is considered to be the most accurate. There is some difference in detail, but no more than is usually encountered when comparing data taken with instruments whose resolving powers are not identical.

TABLE II. Integrated solar spectral irradiance data. The wavelength λ is in angstroms and the zero air mass spectral irradiance H_λ is in μw cm^{-2} A^{-1}. The integrated values were obtained by averaging the detailed solar distribution data over a 100-A interval taking points separated by 10 A.

λ	H_λ	λ	H_λ	λ	H_λ	λ	H_λ	λ	H_λ	λ	H_λ
3080	7.4	3310	11.5	3540	11.6	3770	12.8	4000	15.4	4230	19.2
3090	7.5	3320	11.3	3550	11.7	3780	12.5	4010	16.0	4240	19.0
3100	7.6	3330	11.2	3560	11.6	3790	12.3	4020	16.7	4250	18.9
3110	7.6	3340	11.2	3570	11.5	3800	12.4	4030	17.5	4260	18.7
3120	7.8	3350	11.2	3580	11.5	3810	12.4	4040	18.2	4270	18.4
3130	8.0	3360	11.1	3590	11.5	3820	12.2	4050	18.8	4280	18.2
3140	8.0	3370	11.2	3600	11.6	3830	12.0	4060	19.1	4290	17.9
3150	8.2	3380	11.2	3610	11.7	3840	11.7	4070	19.3	4300	17.8
3160	8.3	3390	11.2	3620	11.9	3850	11.6	4080	19.3	4310	17.7
3170	8.3	3400	11.1	3630	12.2	3860	11.6	4090	19.3	4320	17.8
3180	8.2	3410	11.1	3640	12.6	3870	11.4	4100	19.4	4330	17.8
3190	8.3	3420	11.3	3650	13.0	3880	11.2	4110	19.4	4340	17.9
3200	8.5	3430	11.5	3660	13.1	3890	11.2	4120	19.4	4350	18.2
3210	8.9	3440	11.6	3670	13.3	3900	11.4	4130	19.4	4360	18.6
3220	9.2	3450	11.6	3680	13.4	3910	11.3	4140	19.3	4370	19.0
3230	9.4	3460	11.7	3690	13.3	3920	11.2	4150	19.2	4380	19.4
3240	9.8	3470	11.6	3700	13.3	3930	11.4	4160	19.1	4390	19.9
3250	10.3	3480	11.6	3710	13.2	3940	11.6	4170	19.2	4400	20.2
3260	10.5	3490	11.6	3720	13.2	3950	11.9	4180	19.2	4410	20.6
3270	10.8	3500	11.8	3730	13.2	3960	12.4	4190	19.2	4420	20.9
3280	11.1	3510	12.0	3740	13.2	3970	13.0	4200	19.2	4430	21.1
3290	11.4	3520	12.0	3750	13.2	3980	13.7	4210	19.2	4440	21.3
3300	11.6	3530	11.8	3760	13.1	3990	14.7	4220	19.2	4450	21.5

Since the resolution in Fig. 5 is too fine for easy comparison with earlier work, and the data of Table I are too detailed for many purposes, a low resolution curve was prepared by averaging the curve of Fig. 5 over a 100-A interval, taking points separated in wavelength by 10 A. These averages are presented in Table II, and are shown as the solid curve of Fig. 6. The data of Table I was used to extend the curve to the wavelengths longer than 4450 A. Comparing this curve with the earlier work shown in Fig. 1, the agreement is best with the data of Pettit which are replotted in Fig. 6. Shown also are Stair's latest (1955) results. Comparing the Mount Lemmon results with Pettit and with Stair, below 5000 A the agreement is best with Stair, and to longer wavelengths with Pettit. The results of Stair between 5000 and 7000 A are high, and are not in agreement with any previous work, including his own earlier measurements. Furthermore, they lead to a value of the extra-terrestrial illuminance that is higher than the recent measurement of Karandikar,[23] and most previous solar illuminance measurements.

VII. ATMOSPHERIC ATTENUATION AND OZONE

The vertical atmospheric attenuation coefficient for the total atmosphere above Mount Lemmon is given by the slope of the log current *vs* air mass curve (cf. Fig. 4) for the particular wavelength considered. The

[23] R. V. Karandikar, J. Opt. Soc. Am. 45, 483 (1955).

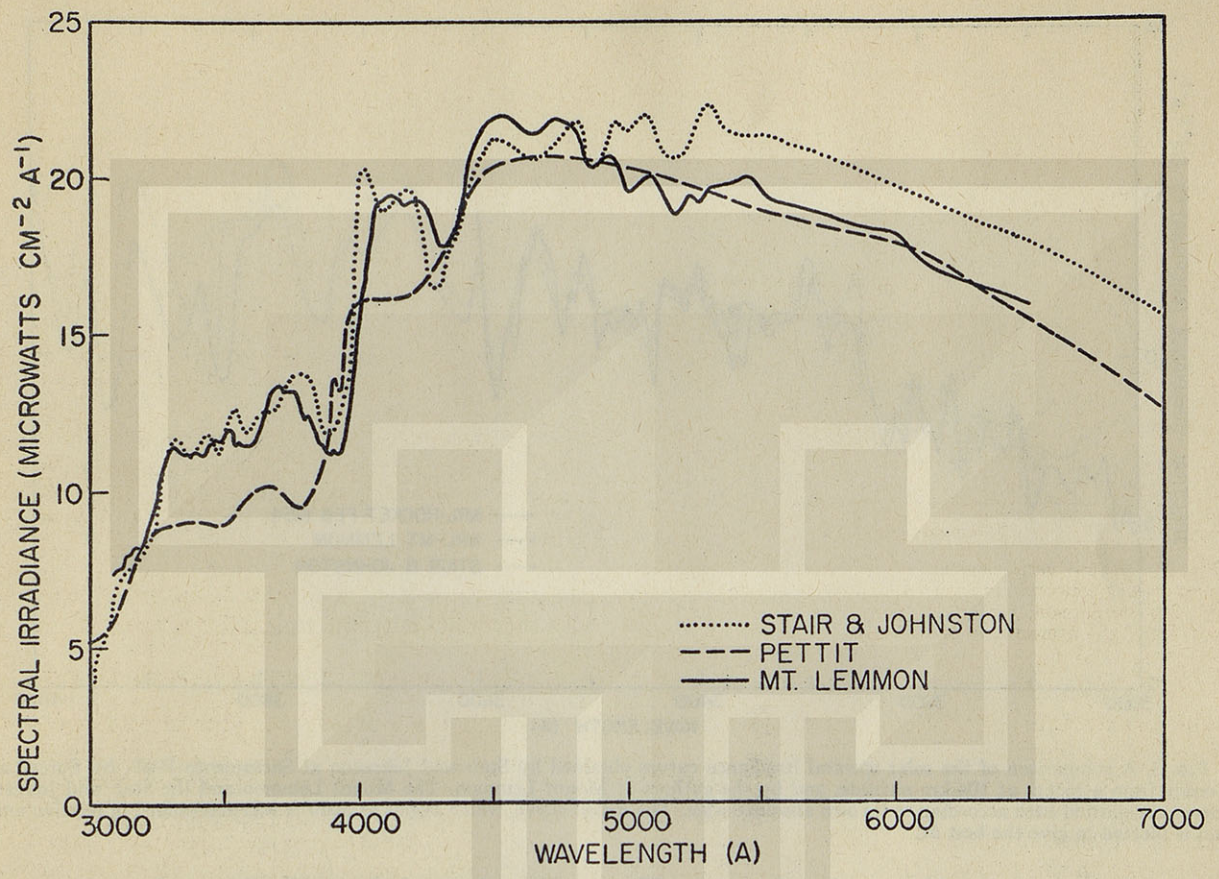

FIG. 6. A comparison of solar spectral irradiance outside the earth's atmosphere obtained by Pettit, by the authors at Mount Lemmon in 1951, and by Stair and Johnston in 1955. The curves below 4500 A have been drawn using (1) the integrated values for the Mount Lemmon data shown in Table II, (2) the integrated distribution as determined by Stair and Johnston, and (3) the Pettit data. For wavelengths longer than 4500 A nonintegrated values are used in each case. The scales of Fig. 6 and Fig. 1 are identical and permit further comparison with the earlier workers.

coefficients listed in Table III, and plotted in Fig. 7, are for the data of the afternoon of October 4, 1951. The attenuation coefficient σ, is defined as the exponential coefficient for the total vertical atmosphere above Mount Lemmon, which has an equivalent thickness of 5.96 km. For comparison, the attenuation curve for a Rayleigh atmosphere of pure air of equivalent thickness 5.96 km is also shown. Use of the log-log plot would make the Rayleigh curve a straight line, except for the small curvature produced by the dispersion of air. The experimental curve departs markedly from the Rayleigh curve in the 4650-A to 7000-A region and also below 3400 A, because of ozone absorption in the Chappuis and Huggins bands, respectively.

From 3400 A to 4650 A, where there is no absorption due to ozone, the observed curve is nearly parallel to, but approximately 15% above the Rayleigh curve. Expressed in terms of the vertical atmospheric transmittance, $e^{-\sigma}$, the atmosphere was approximately 5% more opaque than a Rayleigh atmosphere of pure air. This difference must be ascribed to atmospheric contaminants. So far as we are aware, there have been no cases observed of a perfectly pure Rayleigh atmosphere, at least in recent years. Tousey and Hulburt,[24] from measurements of sky brightness from aircraft at 10 000

TABLE III. Spectral exponential attenuation coefficients of the total vertical atmosphere above Mount Lemmon on October 4, 1951. The wavelength λ is in angstroms and the attenuation coefficient σ is to the base e for an equivalent atmospheric thickness of 5.96 km.

λ	σ	λ	σ	λ	σ	λ	σ
3030	2.54	3301	0.658	3807	0.377	5088	0.132
3032	2.39	3308	0.650	3830	0.361	5174	0.131
3052	2.06	3322	0.644	3848	0.359	5230	0.123
3056	2.04	3330	0.629	3933	0.310	5260	0.118
3078	1.70	3335	0.618	3950	0.308	5312	0.120
3086	1.632	3368	0.584	3968	0.299	5380	0.123
3088	1.591	3380	0.592	4019	0.293	5450	0.124
3116	1.335	3410	0.575	4062	0.279	5525	0.116
3118	1.323	3414	0.562	4094	0.267	5604	0.133
3141	1.121	3442	0.549	4220	0.241	5700	0.112
3152	1.081	3456	0.521	4272	0.228	5758	0.118
3158	1.043	3470	0.526	4300	0.213	5800	0.112
3168	0.960	3508	0.489	4380	0.208	5842	0.098
3182	0.936	3522	0.483	4439	0.203	5980	0.096
3192	0.897	3550	0.471	4546	0.178	6021	0.097
3204	0.849	3585	0.455	4640	0.167	6122	0.081
3212	0.789	3600	0.455	4726	0.159	6280	0.075
3221	0.792	3637	0.437	4808	0.152	6502	0.065
3225	0.811	3683	0.409	4850	0.148		
3242	0.751	3716	0.399	4948	0.137		
3279	0.703	3740	0.392	5002	0.139		

[24] R. Tousey and E. O. Hulburt, J. Opt. Soc. Am. 37, 78 (1947).

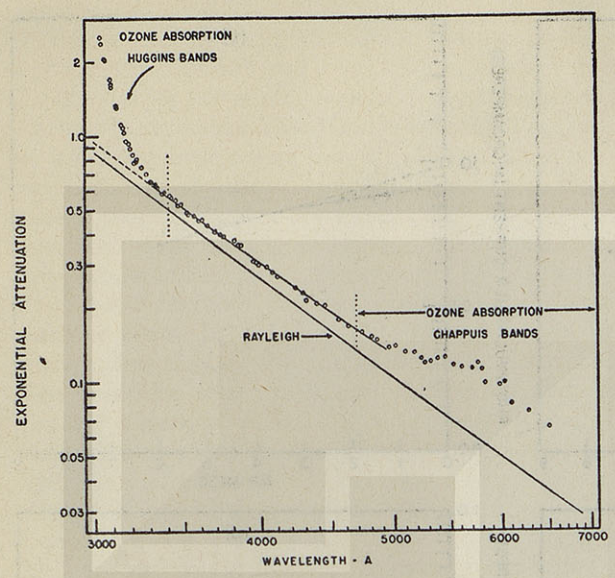

FIG. 7. Spectral vertical attenuation of the total atmosphere above Mount Lemmon from an elevation of 8015 feet on October 4, 1951. For comparison, the attenuation curve for a theoretically pure (Rayleigh) atmosphere of equivalent thickness (5.96 km) is shown.

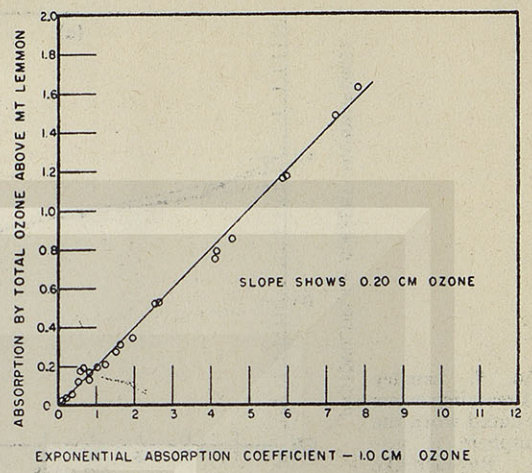

FIG. 8. A plot of the absorption by total ozone above Mount Lemmon *vs* the Ny and Choong exponential absorption coefficients which yields the amount of ozone above Mount Lemmon on October 4, 1951.

ft and Packer and Lock,[25] from similar measurements up to 38 500 ft, concluded that the atmospheric attenuation coefficient for visible light was approximately 35% higher than for pure air at 5500 A. The Mount Lemmon data for October 4, depart from Rayleigh by approximately 30% in this region. The data of Stair at Climax (1951) and of Stair *et al.* from Sacramento Peak (1953) depart even more from Rayleigh.

The amount of ozone present was determined from the absorption in the Huggins band region between 3400 A and 3000 A, and derived from Fig. 7 from the difference between the observed curve and the extrapolation of the nearly linear segment to wavelengths shorter than 3400 A. In Fig. 8 the values of absorption are plotted against the Ny and Choong[26] absorption coefficients, for the various wavelengths in the Huggins region. The points fall on a straight line, as they should, from whose slope the total ozone was determined as 2.00±0.05 mm (NTP).† In the Chappuis band region, absorption by ozone is relatively weak and the accuracy of the data is less because of reduced resolution of the monochromator and diminished sensitivity of the phototube. Therefore, the ozone content cannot be determined with precision from these data. Nevertheless, the absorption in this region using coefficients determined by Vassy and Vassy[27] was found to be consistent with the values expected from 2.0-mm ozone.

VIII. EXTRAPOLATION TO ZERO ATMOSPHERE

Now that the instrumental error in solar measurements can be made very small by present day refinement in techniques, the principal error remaining in determining the solar curve for zero atmosphere is that introduced by the Langley extrapolation procedure, especially if the atmosphere is not uniform and stable. The most accurate extrapolation will be obtained on the day with the clearest atmosphere, this being the best guarantee of homogeneity and stability. Therefore, we have chosen to report final data from the results of the best day only (October 4, 1951). A reduction in accuracy will result from averaging the data of the best day with those obtained on days that were also good, but showed definite signs of changing atmospheric transmission. Data from several less perfect days are also presented to illustrate the manner in which erroneous results may be obtained.

There are two principal criteria that can be applied to determine the constancy of the atmospheric transmission on a given day. The measurements taken on October 4, 1951 will be used in the discussion of these criteria. The first is the straightness of the log energy *vs* air mass (Langley) plots, which are shown in Fig. 4 for three selected wavelengths. In the ideal case, the data for each wavelength would fall on a single straight line from sunrise through noon and back to sunset. The data for both the morning and afternoon runs of October 4 fell exactly on straight lines. There was a small difference in slope between the two sets of runs, showing that the atmospheric attenuation was slightly less in the morning than in the afternoon. However, the extrapolated intersection at zero atmosphere was the

[25] D. M. Packer and C. Lock, J. Opt. Soc. Am. **41**, 473 (1951).
[26] Ny Tsi-Ze and Choong Shin-Piau, Compt. rend. **195**, 309 (1932); **196**, 916 (1933).
† Recently the International Ozone Commission [International Ozone Commission Circular No. 0.4 (July 5, 1957)] adopted the coefficients found in 1953 by Vigroux [E. Vigroux, Annales de Physique **8**, 709 (1953)] and stated that his values have had ample confirmation by independent methods. We used these coefficients and our points again fall along a straight line with a slope yielding a value of 2.43±0.03 mm of total ozone at NTP.
[27] A. Vassy and E. Vassy, J. Chem. Phys. **16**, 1163 (1948).

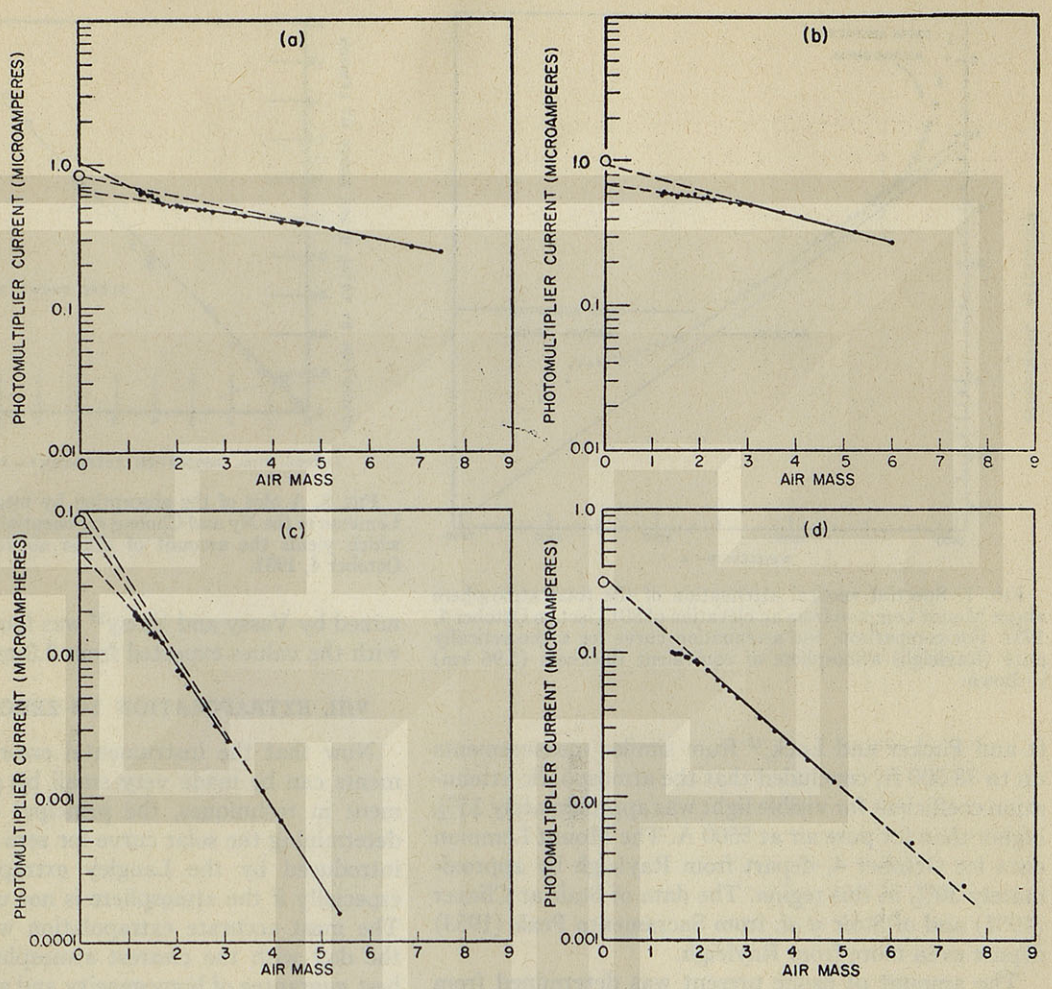

FIG. 9. Langley plots revealing errors introduced when the atmosphere is neither Rayleigh-like nor constant. In each plot there is shown the point for zero atmosphere for the particular wavelength as determined from the October 4, 1951 data.

same for both sets. This is good evidence that no error was introduced because of the slight difference in atmospheric attenuation.

Data reaching large values of air mass are of great importance in establishing valid straight lines. This is particularly true because the sun's altitude is changing rapidly over this range, resulting in a large change of air mass in a short period of time, thereby minimizing the possibility of any significant change in atmospheric attenuation during the measurements. The region near noon, on the other hand, when the air mass is practically constant, is of least value in establishing the extrapolation. In actual measurements, the maximum value of air mass that could be reached, even on a very clear day, depended upon the wavelength. In the visible and down to 3400 A, it was possible to reach $m=12$; while within the Huggins Band region the range was reduced. For the wavelength range below 3400 A, where absorption by ozone becomes important, it was necessary to make a correction for the curvature of the ozone layer, following the method of Dobson.[28] After this was done, these Langley plots were found to be straight lines.

[28] *Operator's Manual for the Dobson Spectrophotometer* (R. and J. Beck, Ltd., London, England).

The second criterion for atmospheric constancy was the plot of atmospheric attenuation *vs* wavelength, Fig. 7. From 3400 A to 4600 A where ozone attenuation is negligible, the lower limit to the attenuation is set by the Rayleigh curve for pure air. The closer the actual attenuation curve lies to the Rayleigh curve, the less the possibility for variation in transmittance due to a changing atmosphere. As previously noted this curve is the closest to Rayleigh that has been obtained to our knowledge, in recent years. Furthermore, the points for the different wavelengths lay on a straight line to within experimental error. This would be expected, because attenuation produced by scattering by ordinary atmospheric contaminants would not show irregular changes over small wavelength intervals, and the known rare absorbing constituents of the atmosphere, such as N_2O, NO, SO_2, NO_2, do not absorb significantly at these wavelengths.

Within the ozone absorption regions the plot of the absorption produced by ozone *vs* the ozone absorption coefficient, Fig. 8, serves as a criterion for the reliability of the results. The straight line obtained checks the correctness of the Langley plots for the several wavelengths.

The types of error introduced when the atmosphere is neither Rayleigh-like nor constant are illustrated by Langley plots for several selected days. Figure 9(a) shows what happens when there is present a suggestion of haze, or perhaps very thin high cirrus. Most of the sky appeared cloudless; however, in sky areas far removed from the sun-to-instrument path, there were a few faint wispy clouds. We always succumbed to the temptation to continue measurements on this type of day, but invariably the data yielded unsatisfactory Langley plots. In the example shown, a single best straight line through the data could not be determined. The point for zero atmosphere determined from the October 4 data is shown, and it can be seen that the data from $m=5$ to $m=7.5$ fall on the correct straight line. However, the points for $m<5$ do not lie on a straight line, and their use would lead to an erroneous value for $m=0$. For example, a solar irradiance value 23% too high would result if the only data collected on this day had been those between $m=1.25$ and $m=2$, whereas the data between $m=2$ and 4.5 would lead to a value 25% low.

Figure 9(b) illustrates data falling on one line for m values less than 3, and on another for the larger values. If one postulates that a single abrupt change in the atmosphere occurred at $m=3$, it should be possible to extrapolate each straight line segment ($m=1.3$ to 3; and $m=3$ to 6) to zero atmosphere and arrive at the same value of solar energy. However, the lines do not meet at $m=0$, and on the basis of this day's run only, it is impossible to decide on the best value for zero air mass. It can be seen, however, that the solar irradiance obtained from extrapolation of the segment between $m=3$ and 6 is within 4% of the indicated correct value based upon the October 4 data, whereas the extrapolation of the measured points at $m<3$ yields results that are 45% low. Inspection of our field notes shows that the sky, though cloudless most of the day, was slightly hazy with some suggestion of inhomogeneity.

Figure 9(c) describes an atmospheric change that appears to have progressed in stages. On the other hand, in Fig. 9(d) the change in atmospheric attenuation seemed to be more continuous. In these cases it is quite apparent that if measurements had been made for low values of m, or for a limited range of m only, straight lines would have been obtained which would have led by extrapolation to incorrect values of the solar intensity for zero atmosphere.

Even if the Langley plots are perfectly straight lines over a wide range of values of m, there is still a possibility that the extrapolated value of solar intensity at $m=0$ may be in error. This possibility arises because σ may vary during the course of the spectral scans in just such a manner that a straight line Langley plot will still be obtained. but this straight line is rotated so as to intersect $m=0$ at an incorrect value of I_0. Consider Eq. (1), which may be rewritten in the form

$$\ln(I/I_0)=-\sigma m. \tag{3}$$

Since we are considering only observations for which straight lines are obtained, that is, for which:

$$\ln(I/I_0)=-am+b,$$

we may compare these expressions, obtaining

$$\sigma=a-b/m. \tag{4}$$

Thus a straight line will result not only when σ is constant ($b=0$), but also when b is not zero. The latter, of course, will lead to the erroneous extrapolation values of solar intensities. However, since, the variation in σ must follow this specific and highly improbable function of m, we are probably safe in disregarding this possibility, provided that measurements are not made over too limited a range of air masses. And once again this emphasizes the importance of the use of the clearness of the sky as the best criterion for the constancy and uniformity of the atmosphere.

The applicability of the Langley method has been criticized by Deirmendjian and Sekera,[29] largely on the basis of the work of the Smithsonian and of Pettit. Their argument is that values of atmospheric transmission were reported that were somewhat greater than the corresponding values for a theoretical pure Rayleigh atmosphere. In the case of the Smithsonian results, this commenced at about 4000 A and increased to short wavelengths. Deirmendjian and Sekera explained this by assuming that a large amount of light was produced by Mie scattering from the sky around the sun and was accepted by the equipment. Our explanation for this is that the greater-than-Rayleigh transmittances were caused by the presence of instrumental stray light. In the Smithsonian work, only a single dispersing monochromator was used. The detector was a bolometer. These are conditions that would produce such an effect. Stray light would also explain the low values for extraterrestrial irradiance reported by the Smithsonian in the ultraviolet.

In the case of the work of Pettit, values of transmittance greater than Rayleigh occurred in the 1934 Mount Wilson fifteen-day mean data below about 4000 A, and persisted to 3300 A, beyond which the attenuation caused by ozone makes it meaningless to compare the results with Rayleigh. The departure from Rayleigh is a small one, but it cannot be explained as caused by instrument stray light because a double dispersing system was used. Inspection of Pettit's published Langley plots for June 8, 1939 suggests, however, that these departures are not significant, since the five points obtained at each wavelength rarely lie on the straight line required to give a precise value of transmittance. It is also quite likely that among the

[29] D. Deirmendjian and Z. Sekera, J. Opt. Soc. Am. 43, 1158 (1953); 46, 565 (1956).

15 days there may have been included seemingly good days when the atmospheric transmittance was actually varying, such as we encountered so frequently at Mount Lemmon. These could easily have led to false values of average transmittance.

Deirmendjian and Sekera have concluded that there is a trend toward higher values of the extra-terrestrial energy as the elevation of the observation station increases, and have suggested that the NRL rocket and Mount Lemmon data, which do not conform, are too low. Their conclusions were based not only upon the Smithsonian work (Mount Wilson and Mount Whitney) and the Pettit work (1934 Tucson) but also upon the earlier work of Stair and co-workers (Sacramento Peak, 1953, and Climax, 1951). Since the more recent (1955) ultraviolet results of Stair and Johnston, the rocket and Mount Lemmon data are in agreement, it would appear that there is little justification for their conclusions.

IX. SOLAR ILLUMINANCE

The solar illuminance outside the atmosphere was determined by multiplying the absolute spectral-irradiance curve from the Mount Lemmon measurements (Fig. 6) by the CIE Standard Luminosity Curve and integrating the area under the resulting curve. This yielded 0.0201 light watts cm^{-2}. Converting to units of illuminance by using 680 lu/w, the reciprocal of the mechanical equivalent of light, we obtained a value of the solar illuminance outside the atmosphere of 12 700 $\pm$400 lumens ft^{-2}. This supersedes the preliminary value 11 500 reported by Dunkelman and Scolnik,[30] the change being caused by the adoption of Johnson's value of the solar constant, as described earlier. The estimated error includes the probable error in solar constant reported by Johnson. It is noted that this result is in agreement with the recent work of Karandikar, who computed the solar illuminance from measurements of the luminance of the solar disk. The value obtained was 12 200$\pm$300 lumens ft^{-2}.

The efficiency ϵ of the sun in producing visible light may be defined as the ratio of the solar illuminance expressed in light watts cm^{-2} to the total solar irradiance which is the solar constant expressed in watts cm^{-2}, whence

$$\epsilon = 0.0201/0.1394 = 0.144.$$

This value is dependent only upon the solar spectral intensity distribution and the CIE Standard Luminosity curve. It is independent of the absolute value of the solar constant and of the value of the mechanical equivalent of light.

[30] L. Dunkelman and R. Scolnik, J. Opt. Soc. Am. 42, 876 (1952).

ACKNOWLEDGMENTS

We wish to express our thanks to Dr. Richard Tousey, in whose group this work was conducted, for his many helpful suggestions and to Francis S. Johnson who suggested this investigation. We are grateful also to the U. S. Forest Service, the Steward Observatory, and the Trico Electric Cooperative of Tucson for aid in determining the location for the experiment and for providing the necessary facilities. Finally our thanks are extended to Helen Gish Drake of Summerhaven Lodge and to Forest Ranger John Brinkley for their cooperation.

Reprinted from JOURNAL OF THE OPTICAL SOCIETY OF AMERICA, Vol. 45, No. 3, 166–175, March, 1955
Printed in U. S. A.

Horizontal Attenuation of Ultraviolet Light by the Lower Atmosphere

WILLIAM A. BAUM* AND LAWRENCE DUNKELMAN
Naval Research Laboratory, Washington, D. C.

(Received September 27, 1954)

The horizontal attenuation of ultraviolet light by the air near the ground was determined as a continuous function of wavelength from 2300 to 4600 A. Measurements were made by means of photographic spectrophotometry on seventy-eight nights during 1949 at Pasadena, California, and also on three nights during 1950 at Washington, D. C. The results are given in the form of a table of attenuation coefficients (km^{-1}) at selected wavelengths and in the form of representative spectral attenuation curves for conditions ranging from fog to exceptionally clear air. Except for weak oxygen absorption bands between 2421 and 2700 A, the attenuation coefficient was found to vary quite smoothly (though differently) with wavelength on all nights. Air pollutants, though frequently present, were not spectroscopically identified except for sulfur dioxide, which was encountered in measurable concentration in Washington. Ozone concentrations could be estimated from a few spectra obtained in exceptionally clear weather.

INTRODUCTION

A BEAM of light, passing through air, is attenuated both by scattering and by absorption. The fraction of its intensity transmitted through x kilometers of homogeneous air is given by $e^{-\sigma x}$, where σ represents the total attenuation per kilometer and is a function of wavelength λ. Therefore, the attenuation of light by a particular sample of air can conveniently be described by plotting σ against λ for the spectral region of interest. No two samples of air behave exactly alike, and the range of possible variation is extremely large. Values of σ at the same wavelength for two samples of air can easily differ by a factor of 100. Moreover, two samples of air having the same σ at one wavelength frequently have quite different values at another.

Previous studies of ultraviolet attenuation in the lower atmosphere as a function of wavelength have been made by several investigators. Spectrographs and line-emission light sources were employed by Schaeffer[1] in 1922, by Dawson, Granath, and Hulburt[2] in 1929, by Buisson, Jausseran, and Rouard[3] in 1930 and 1934, by Götz and Maier-Leibnitz[4] in 1933, and recently by Curcio *et al.*[5] A spectrally continuous light source was used in conjunction with a spectrograph by Vassy and Vassy[6] in 1939 and by A. Vassy[7] in 1941. Color filters and photoelectric receivers were used by Koch[8] in 1943. For the most part, the results of these various investigations involved limited sampling and pertained to very clear air or to haze of uncertain description.

The principal aim of the present study was to determine ultraviolet attenuation coefficients under a wide variety of air conditions and to seek correlations with the measured visual range. Measurements were obtained on seventy-eight representative nights[9] during 1949 at the California Institute of Technology in Pasadena and on three nights during 1950 at the

* At the California Institute of Technology during the first portion of this work and now at Mount Wilson and Palomar Observatories, Pasadena 4, California.

[1] E. R. Scheaffer, Proc. Am. Acad. Arts Sc. 57, 365 (1922).

[2] Dawson, Granath, and Hulburt, Phys. Rev. 34, 136 (1929).

[3] Buisson, Jausseran, and Rouard, Compt. rend. 190, 808 (1930); 194, 1477 (1934).

[4] F. W. P. Götz and H. Maier-Leibnitz, Z. Geophys. 9, 253 (1933).

[5] Curcio, Drummeter, Petty, Stewart, and Butler, J. Opt. Soc. Am. 43, 97 (1953).

[6] A. Vassy and E. Vassy, J. phys. 10, 75, 403, 459 (1939).

[7] A. Vassy, thesis, University of Paris, 1941.

[8] B. Koch, Optik 5, 258 (1949).

[9] W. A. Baum, Thesis, California Institute of Technology, 1950.

Naval Research Laboratory in Washington, D. C. Forty-five of the seventy-eight Pasadena nights were consecutive. Visual ranges (defined below) of 0.4 km to 100 km were encountered among the eighty-one air samples investigated.

Another aim was to examine, by use of a continuous spectrum source, the role played by line or band absorption in the atmosphere, so as to make certain that simple methods of measuring atmospheric attenuation in the ultraviolet using line spectrum sources do not give misleading results. Vassy and Vassy,[6] and A. Vassy[7] observed oxygen and ozone bands in exceptionally clear air with a continuous source and spectrograph; an extension of the work to other types of atmospheres was required.

A description of the methods and results of the present work should be prefaced by some remarks pertaining to: (1) the factors which contribute to attenuation, (2) the relation between daylight visual range and attenuation, and (3) the influence of optical geometry on attenuation measures.

For air near the earth's surface, three factors contribute to attenuation, and the total coefficient is the sum of the coefficients for the individual contributors. Thus, we may write

$$\sigma=\sigma_A+\sigma_B+\sigma_C, \tag{1}$$

where σ_A is the component due to Rayleigh scattering by air molecules, σ_B represents scattering and absorption by air-borne particles and droplets, and σ_C is absorption by gases.

Molecular scattering, treated by Rayleigh[10] and others,[11–15] was applied by Tousey and Hulburt[16] in the form:

$$\sigma_A=\frac{8\pi^3(n-1)^2}{3N\lambda^4}\cdot\frac{6(1+\rho)}{6-7\rho}\cdot\left[3+\frac{1-\rho}{1+\rho}\right]10^5\ \mathrm{km}^{-1}, \tag{2}$$

where λ is the wavelength in centimeters, n is the refractive index of air (function of λ), N is the number of gas molecules per cubic centimeter, and ρ is the polarization defect for light scattered at $\pi/2$. According to Born,[17] this polarization defect for air molecules is about 0.04 throughout the optical spectrum. It influences σ_A by only a few percent. For 0°C at sea level (760 mm pressure), Eq. (2) reduces to

$$\sigma_A=(1.32\cdot10^{-12})\frac{(n_0-1)^2}{\lambda^4}\mathrm{km}^{-1}. \tag{2a}$$

Molecular scattering alone falls far short of accounting for the total attenuation of light by the lower atmosphere, even in relatively clear weather. In regions of the spectrum where gas absorption plays no major role, the attenuation σ_B due to scattering and absorption by air-borne particles and droplets generally predominates. The relation between σ_B and λ depends upon the particle population and size distribution, and a wide variety of conditions can occur.

Empirical studies of spectral scattering by artificial fogs have been made by Houghton[18] and by Nukiyama and Kobayasi.[19] In both experiments the (σ,λ) curve was found to have humps instead of following the form of λ^{-n}. The theory of spectral scattering by small particles was first developed by Mie.[20] The work of Stratton and Houghton,[21] based on the theory of Mie, showed that the attenuation coefficient σ is not necessarily a function that decreases monotonically with increasing λ; thus the experimentally observed humps for artificial fogs could be interpreted theoretically by assuming a suitable distribution of particle sizes. Tables of scattering functions have been published by the National Bureau of Standards[22] and by Gumprecht *et al.*[23] and further detail has been discovered by the computations of Goldberg and Penndorf.[24]

The absorption of radiation by gas molecules σ_c is more commonly associated with the infrared and the far ultraviolet than with the visible region or the near ultraviolet. Within the spectral region covered by the present observations the only prominent absorptions by natural gases of the air are those due to ozone and oxygen. Certain pollutants including sulfur dioxide also have weak absorption bands in this region.

The small quantity of ozone, presumably carried into the lower atmosphere from upper layers where it is formed, has been the topic of several investigations.[25–31] Its absorption is a broad continuum extending from roughly 2000 A to 3000 A with its maximum around 2500 A.

Atmospheric oxygen[32] is responsible for an absorption

[10] Lord Rayleigh, Phil. Mag. 41, 107 (1871) and ff. Also in *Scientific Papers* (Cambridge University Press, Cambridge, 1899), Vol. I, pp. 87–103.
[11] M. v. Smoluchowski, Ann. Physik. 25, 205 (1908).
[12] A. Einstein, Ann. Physik. 33, 1275 (1910).
[13] J. Cabannes, *La Diffusion Moleculaire de la Lumiere* (Presses Universitaires, Paris, 1929).
[14] W. H. Martin and S. Lehrman, J. Phys. Chem. 26, 75 (1922).
[15] L. H. Dawson and E. O. Hulburt, J. Opt. Soc. Am. 31, 554 (1941).
[16] R. Tousey and E. O. Hulburt, J. Opt. Soc. Am. 37, 78 (1947).
[17] M. Born, *Optik* (J. Springer, Berlin, 1933).
[18] H. G. Houghton, Phys. Rev. 38, 152 (1931).
[19] D. Nukiyama and A. Kobayasi, Tokyo Univ. Aeronaut. Research Inst., Report No. 82, (1932).
[20] G. Mie, Ann. Physik. 25, 377 (1908).
[21] J. Stratton and H. G. Houghton, Phys. Rev. 38, 159 (1931).
[22] *Tables of Scattering Functions for Spherical Particles* (National Bureau of Standards Applied Mathematics Series 4, U. S. Government Printing Office, Washington, D. C., 1948).
[23] Gumprecht, Sung, Chin, and Sliepcevich, J. Opt. Soc. Am. 42, 226 (1952).
[24] B. Goldberg and R. Penndorf, Bull. Am. Meteorol. Soc. 34, 379 (1953).
[25] C. Fabry and H. Buisson, Compt. rend. 192, 457 (1931).
[26] Götz and Ladenburg, Naturwiss. 19, 373 (1931).
[27] Götz, Schein, and Stoll, Gerl. Beitr. Geophys. 45, 237 (1935).
[28] D. Chalonge and E. Vassy, J. phys. 5, 309 (1934).
[29] R. Auer, Gerl. Beitr. Geophys. 54, 137 (1939).
[30] Ny Tsi-Ze and Choong Shin-Piaw, Compt. rend. 195, 309 (1932); 196, 916 (1933).
[31] L. P. Granath, Phys. Rev. 34, 1045 (1929).
[32] R. A. Craig, "The Observation and Photochemistry of Atmospheric Ozone and their Meteorological Significance," Meteorological Monographs, Am. Meteorol. Soc. (1950).

which commences around 2700 A and rises toward shorter wavelengths; it sets the lower wavelength limit at about 2300 A for the path lengths employed in the present work. Below this limit, the absorption continues to rise until it renders the air almost totally opaque around 1850 A for paths longer than a few millimeters. Contributing to the absorption between 2700 A and 2421 A are the Ciechomski bands[33,34] (also called the Herzberg bands) which have been studied in outdoor air by Chalonge and Vassy[35] and in the laboratory by Herzberg.[36]

The relation between the horizontal daylight visibility and the scattering components of attenuation, given originally by Koschmieder[37] and described by Hulburt[38] and by Middleton,[39] is

$$V\bar{\sigma}=\ln\frac{1}{\eta}, \tag{3}$$

where V is the horizontal visual range, $\bar{\sigma}$ is the effective scattering coefficient for daylight as seen by the human eye, and η is the visual threshold of brightness contrast. Since η is normally taken as 0.02, Eq. (3) becomes

$$V\bar{\sigma}=3.91. \tag{3a}$$

In the visible spectrum, scattering predominates over absorption; hence, this $\bar{\sigma}$ is about the same as the total attenuation coefficient σ for an effective visual wavelength (say 5500 A). Horizontal visual ranges defined by Eq. (3a) were useful to the present problem in that they provided a handy tag for labeling air samples whose spectral attenuation curves (σ,λ) were being measured.

It is evident that the optical geometry of a system designed to measure attenuation must be arranged so as to exclude from the receiver light which is scattered by the air surrounding a terrestrial source. Errors due to this effect have been investigated for the visible spectrum by Middleton[40] and by Stewart and Curcio.[41] In the present investigation, most of the spectral attenuation data were obtained with apparatus having a source cone which was masked down to two minutes of arc while the field of view of the receiver was less than a half-degree. This arrangement effectively reduced the scattering error to negligible proportions.

EXPERIMENTAL PROCEDURES

In the preceding section several factors are mentioned which influenced the design of the apparatus. These included: (1) the desirability of extensive sampling, (2) the advantages of detailed spectral resolution, and (3) the necessity for employing a narrow source beam and a narrow field of view at the receiver. To these we may add (4) the importance of minimizing exposure times so as to obviate effects due to changing meteorological conditions and (5) the selection of optimum path length for the spectral region involved.

The optical system used for more than 90 percent of the attenuation measurements reported in this paper is diagrammed schematically in Fig. 1. Basically it consisted of a light source with suitable projection optics, an arrangement of front-surface mirrors to fold part of the light into two paths of different length, and a quartz objective spectrograph (Fig. 2) which photographed both reflected beams simultaneously.

The folding of the paths and the use of remote electrical controls enabled one person to operate the entire system and thereby greatly facilitated extensive sampling. The spectrograph provided adequate spectral resolution and it possessed a very narrow effective field of view which, together with suitable source-beam limitations, obviated errors due to accepting scattered light. Initial experiments demonstrated that there would be no difficulty in obtaining enough light for short exposures and that a path difference of several hundred meters was suitable.

The light source was a 500-watt high pressure xenon dc arc lamp. Its general characteristics have been described by Schulz[42–44] and its ultraviolet properties have been reported by Baum and Dunkelman.[45] The lamp radiates a smooth ultraviolet continuum, which extends to 2200 A and is interrupted by only a few weak lines. The ultraviolet radiance of the arc nucleus exceeds that of most other ultraviolet-continuum sources including a carbon crater. Because of its compactness, its rich clean continuum, and its stability, the high pressure xenon arc was ideally suited for this work.

A schematic diagram of the quartz objective spectro-

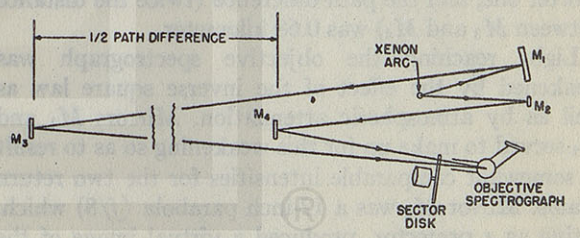

FIG. 1. Schematic diagram (not to scale) of the folded-path optical system used in conjunction with the high pressure xenon arc for most of the atmospheric attenuation measurements. Remote electrical controls enabled one person to operate the entire system and thereby facilitated extensive sampling of various atmospheric conditions.

[33] A. Ciechomski, dissertation, Universität Freiburg (Switzerland), 1910.
[34] O. R. Wulf, Proc. Natl. Acad. Sci. 14, 609 (1928).
[35] D. Chalonge and E. Vassy, Compt. rend. 198, 1318 (1934).
[36] G. Herzberg, Naturwiss. 20, 577 (1932).
[37] H. Koschmieder, Naturwiss. 26, 521 (1938).
[38] E. O. Hulburt, J. Opt. Soc. Am. 31, 467 (1941).
[39] W. E. K. Middleton, *Vision through the Atmosphere* (University of Toronto Press, Toronto, Canada, 1952).
[40] W. E. K. Middleton, J. Opt. Soc. Am. 39, 576 (1949).
[41] H. S. Stewart and J. A. Curcio, J. Opt. Soc. Am. 42, 801 (1952).
[42] P. Schulz, Zeits. Naturfor. 2a, 583 (1947).
[43] P. Schulz, Ann. phys. 6, 95, 107 (1947).
[44] P. Schulz, Reichsber. Physik 1, No. 5, 147, April 1944.
[45] W. A. Baum and L. Dunkelman, J. Opt. Soc. Am. 40, 782 (1950).

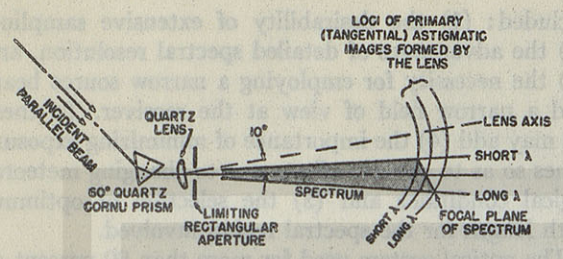

FIG. 2. Optics of the quartz objective spectrograph. Astigmatism introduced by the tilted lens resulted in spectra suitably widened for microphotometry.

graph is shown in Fig. 2. This instrument, constructed by the U. S. Weather Bureau, was patterned somewhat after the one described by Chalonge and Vassy.[46] Nearly parallel light from the two distant source images was incident upon a 60° quartz Cornu prism of 40 mm height. Just behind the prism was a plano-convex singlet quartz lens with a nominal focal length of 500 mm. By orienting this lens as shown in the figure, one can introduce astigmatism to widen the spectrum of a point source and thereby make it suitable for microphotometry. If the photographic emulsion is placed at the loci of primary astigmatic images for the various wavelengths, the resulting spectrum has nearly the appearance of a spectrum formed by an ordinary slit spectrograph, except that it is wedge-shaped. The dispersion of this instrument was roughly 15 A per mm at 2200 A, 60 A per mm at 3500 A, and 200 A per mm at 5000 A.

The various components in Fig. 1 were housed in three stations mounted on the roofs of buildings at the California Institute of Technology campus at an elevation of 250 meters above sea level. In addition to the xenon arc lamp and the objective spectrograph, the main station included mirrors M_1 and M_2, a rotating sector disk, and various electrical controls for remote manipulation of shutters protecting the path-folding mirrors M_3 and M_4 located at the other two stations. The long path was roughly ten times the shorter one, and the path difference (twice the distance between M_3 and M_4) was 0.68 kilometer.

Light reaching the objective spectrograph was weakened by the effect of the inverse square law as well as by atmospheric attenuation. Mirrors M_1 and M_2 served to make up for this weakening so as to result in somewhat comparable intensities for the two return beams. Mirror M_1 was a 12-inch parabola ($f/8$) which, acting as a projector, produced a virtual image of the whole xenon-arc stream enlarged about 10 times. Mirror M_2, a 4-inch optical flat, was introduced to make the number of reflections in the two paths equal. The lamp itself was obscured from direct view so that only the two reflected beams were involved. The path-folding mirrors, M_3 and M_4, were 8-inch optical flats located in the same vertical plane as the spectrograph aperture, although to avoid confusion they are diagrammed differently in Fig. 1. Thus, the objective spectrograph received the two beams simultaneously, and the spectra were formed one just above the other. The two beams, each subtending 10 seconds of arc, were about a half-degree apart.

Neglecting back scattering compared with forward scattering, one may regard the 8-inch apertures of the path-folding mirrors as source-cone diaphragms which prevent errors due to receiving extraneous scattered light. For the long path, the source cone was thus limited to less than 2 minutes of arc; for the short path, the distance was too small for scattering to be important. As one would expect from geometry, the projected source cones attained a 16-inch diameter when they reached the spectrograph, where they were centered upon an entrance aperture 20 by 33 mm. All mirrors were ruggedly mounted and were provided with accurate means of alignment (especially M_3) so that optical readjustment was rarely required.

Dancing shadow patterns caused by atmospheric boil in the longer path were of small dimensions compared with the 16-inch beam and were obviously rapid enough to be averaged out over any exposure exceeding a duration of several seconds.

Just ahead of the spectrograph, the return beams were chopped about 100 times per second by a rotating sector disk whose angular opening could be set at 30 percent, 10 percent, 3 percent, and 1 percent. To obtain 100 percent exposure, the chopper was removed. To obtain 0.3 percent and 0.1 percent, the spectrograph aperture was cut to 10 percent of its full width while the 3 percent and 1 percent sector settings were repeated. Thus the complete sequence consisted of seven logarithmically distributed exposures ranging from 100 percent down to 0.1 percent in relative value, but all of equal duration. Exposures of 10 seconds were found to yield a sequence of spectra having a suitable range of photographic densities (see Fig. 3). At the same time they were short enough to obviate difficulties due to variations in local meteorological conditions but long enough to integrate variations due to atmospheric boil. In order to time the 10-second exposures with accuracy, the spectrograph was equipped with an electrically actuated shutter connected in series with an electric timer; in this manner, timing errors were held under 0.5 percent.

Except for a few special experiments, all spectra were photographed on Eastman 103-0 film having a black antihalation backing and a fluorescent front coating. These were brush-developed under controlled conditions.

It was necessary to monitor from time to time the "vacuum" transmission ratio of the system; that is, the relative intensities of the pairs of spectra that would have been obtained had the air been completely transparent. For this purpose the three auxiliary systems of attenuation measurement employed oc-

[46] D. Chalonge and E. Vassy, Rev. optique 13, 113 (1934).

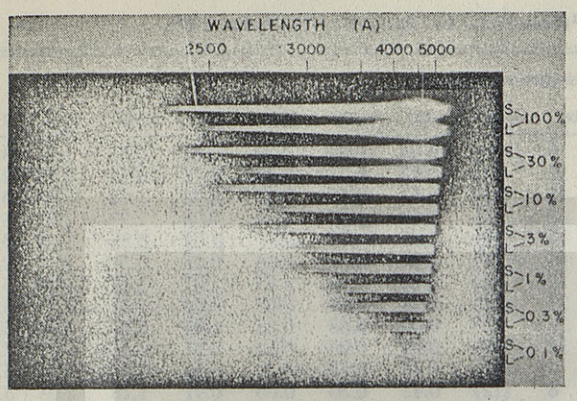

FIG. 3. A typical sequence of atmospheric transmission spectra obtained with the xenon-arc optical system (Fig. 1) on a clear night (August 22, 1949) at Pasadena when the visibility range was about 100 km. The spectra marked *S* represent the short path while those marked *L* represent the long path; relative exposures (see text) of the seven pairs are labeled in percent. The Ciechomski oxygen bands can be seen in the 2500-A region of the long-path spectra. Features around 4500 A are weak lines in the source.

casionally were (1) ultraviolet spectra obtained using a portable light source, (2) "haze-meter" readings at 5500 A, and (3) cadmium photocell readings of 2537-A radiation from a mercury arc. The first of these yielded spectrally continuous attenuation data over the same spectral region covered by the xenon-arc system, while the second and third systems each provided a check point of one wavelength.

The optical system utilizing a portable light source is shown schematically in Fig. 4. A 50-watt Nestor hydrogen-arc lamp of the type described by Allen and Franklin[47] was carried first to the same distance as mirror M_3 and then to that of mirror M_4. No mirror was used, and the path difference was effectively half that of the folded-path system. Spectra were photographed with the objective spectrograph using the sector disk as before, except that (1) exposures of 1000 seconds duration were required, (2) the long-path and short-path exposures could not be simultaneous without introducing unwanted complications, and (3) the difference in illumination due to the inverse square law was counterbalanced by using different sector settings for the two paths instead of by using optical magnification. Two pairs of hydrogen-arc spectra were added to a standard xenon-arc sequence on each of six nights in Pasadena.

On the three nights when attenuation measures were made at Washington, D. C., the hydrogen-arc system was used by itself. Not only did this system require no auxiliary calibration, but it also involved less total effort than a folded-path arrangement where a limited number of nights were to be sampled. A 8-inch focal length quartz lens was used in conjunction with the arc at its more distant location, and was adjusted to increase the effective intensity by a factor of 10. The path difference was 0.9 km and the elevation was 20 meters above sea level.

In order to estimate the attenuation coefficient σ at 5500 A, readings were taken with a British Admiralty haze-meter known as the Lo)fah[48] on twenty of the eighty-one nights investigated. This instrument is a box, about the size of a foot locker, having a self-contained optical system. Baffled vents permit outside air to circulate freely through the box. The amount of light scattered at 30° from an intense light beam is matched visually against a variable comparison field; settings of the latter yield values which are a measure of $\bar{\sigma}$ as used in connection with Eq. (3) and (3a).

Monochromatic measurements of σ at 2537 A were obtained on six of the eighty-one nights using a portable cadmium photocell photometer and an array of twelve 30-watt "slim-line germicidal" mercury lamps. A cadmium photocell is sensitive only to the region from 2100 A to 2900 A, and lamps of the type used radiate more than 99 percent of their energy at 2537 A. The photometer, which was a more sensitive and more stable version of the unit described by Haynes and Taylor,[49] was equipped with a 4-inch quartz collecting lens. An attached sighting telescope facilitated reproducibility in aiming it at the lamp array.

DATA REDUCTION

Figure 3 shows a typical sequence of atmospheric transmission spectra obtained on a clear night (August 22, 1949) when the visibility range as defined by Eq. (3a) was 100 km. As for most nights, the light source was the high pressure xenon arc, and the sequence consisted of seven 10-second exposures ranging from 100 percent to 0.1 percent in relative value as already described. The upper spectrum of each of the seven pairs in Fig. 3 represents the short path, while the lower spectrum represents the long path. Since this night was quite clear, the densities of the long- and short-path spectra are similar in the visible region; whereas in the ultraviolet, say at 2500 A, there is a large difference in density due to the greater attenuation at that wavelength than in the visible region. In the long-path spectra the Ciechomski bands of O_2 can be seen around 2500 A.

Spectra produced by both the xenon-arc and the

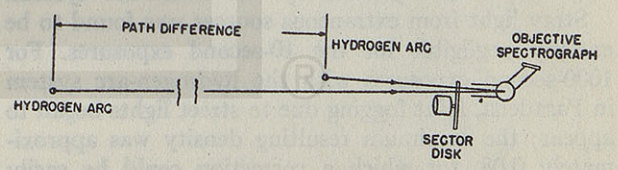

FIG. 4. Schematic diagram (not to scale) of the optical system employing a portable hydrogen arc. Although this system involved neither the preparation nor calibration required by a folded-path system, it needed more than one operator and it consumed more time per measurement.

[47] A. J. Allen and R. G. Franklin, J. Opt. Soc. Am. **29**, 453 (1939).

[48] British Ministry of Home Security Report RC(G) 43, (1943).

[49] A. H. Taylor and H. Haynes, Gen. Elec. Rev. 50, 27, (1947).

TABLE I. Spectral attenuation coefficients, σ km^{-1}(base e) for air, Pasadena, California, 1949.

Date	V (km)	Wavelength in angstroms 4300	4000	3600	3200	2900	2620	2400
Mar. 31	19	0.32	0.43	0.57	0.76	1.05	1.51	3.19
Apr. 1	23	0.20	0.25	0.33	0.50	0.81	1.26	2.85
2	7	1.10	1.38	1.51	1.89	2.17	3.07	4.77
3	16	0.52	0.59	0.69	0.92	1.21	2.06	3.75
4	15	0.38	0.49	0.57	0.88	1.22	1.98	3.91
5	6	1.44	1.61	1.74	2.30	2.72	3.74	4.78
6	50	0.11	0.08	0.07	0.27	0.50	1.31	2.69
7	25	0.50	0.57	0.60	0.80	1.07	1.65	3.63
8	15	0.46	0.50	0.71	0.97	1.25	1.96	3.78
9	19	0.27	0.35	0.45	0.70	0.95	2.00	3.63
10	22	0.23	0.38	0.40	0.65	0.89	1.61	3.31
11	14	0.44	0.52	0.75	0.96	1.46	2.40	3.96
12	(10)	0.61	0.67	0.69	0.96	1.13	1.64	3.28
13	(24)	0.26	0.23	0.32	0.56	0.71	1.38	2.87
14	(12)	0.41	0.47	0.66	0.85	1.10	1.67	3.30
15	(12)	0.44	0.49	0.63	0.83	1.07	1.74	3.47
16	(39)	0.16	0.17	0.19	0.33	0.63	1.27	2.70
17	(19)	0.30	0.36	0.45	0.63	0.85	1.29	2.69
18	(4)	1.30	1.50	1.65	1.78	2.09	2.64	4.17
19	(17)	0.38	0.48	0.49	0.69	0.89	1.39	3.21
20	(8)	0.73	0.98	1.11	1.44	1.96	2.72	4.47
21	(7)	0.76	0.91	1.09	1.43	1.95	2.63	4.30
22	(7)	0.85	1.03	1.14	1.53	2.02	2.49	4.61
23	(2)	2.33	2.27	2.51	2.76	3.01	4.04	5.02
24	(4)	1.41	1.69	1.70	2.06	2.53	3.50	4.87
25	(6)	0.92	1.07	1.16	1.25	1.69	2.90	4.34
26	(8)	0.80	0.96	0.96	1.20	1.37	2.31	3.74
27	(6)	0.87	0.99	1.10	1.34	1.66	2.26	4.38
28	(30)	0.19	0.24	0.34	0.65	0.87	1.48	3.20
29	(21)	0.28	0.32	0.46	0.52	0.79	1.27	2.82
30	(18)	0.28	0.49	0.60	0.84	1.09	2.12	3.47
May 1	(16)	0.39	0.42	0.46	0.65	1.01	1.97	2.98
2	(13)	0.43	0.53	0.60	0.81	1.11	1.74	3.24
3	(80)	0.07	0.11	0.18	0.34	0.66	1.26	2.72
4	(30)	0.19	0.26	0.30	0.44	0.70	1.23	2.84
5	(8)	0.71	0.93	0.93	1.26	1.60	2.54	4.63
6	(100)	0.03	0.06	0.17	0.29	0.62	1.48	3.03
7	(15)	0.37	0.39	0.58	0.80	1.09	1.84	3.62
8	(50)	0.11	0.13	0.22	0.39	0.73	1.18	2.73
May 9	(100)	0.06	0.14	0.30	0.47	0.71	1.61	3.11
May 10	(44)	0.12	0.17	0.25	0.47	0.70	1.40	2.87
11	(10)	0.53	0.59	0.77	0.92	1.18	2.05	3.41
12	(9)	0.59	0.65	0.76	0.90	1.23	1.87	3.55
13	(24)	0.22	0.25	0.37	0.62	0.86	1.62	3.03
14	(100)	0.04	0.09	0.18	0.35	0.54	1.18	2.64
18	(2)	1.78	1.79	1.88	2.07	2.41	3.09	4.04
23	(12)	0.44	0.54	0.65	0.96	1.38	1.97	3.69
27	(9)	0.60	0.68	0.83	1.04	1.29	2.03	3.51
31	(100)	0.04	0.06	0.12	0.37	0.61	1.04	2.91
June 6	(11)	0.46	0.58	0.79	1.10	1.38	2.06	3.77
8	(12)	0.42	0.50	0.60	0.91	1.18	2.08	3.28
13	(6)	0.87	0.90	1.07	1.31	1.62	2.42	...
16	(12)	0.43	0.48	0.52	0.81	1.02	1.74	...
21	(16)	0.36	0.37	0.44	0.74	1.05	1.67	3.51
27	(44)	0.13	0.15	0.30	0.47	0.72	1.49	3.35
July 1	(4)	1.17	1.23	1.68	2.06	2.53	3.56	...
7	(11)	0.51	0.63	0.68	0.86	1.18	1.86	3.21
14	(8)	0.63	0.72	0.99	1.41	1.80	2.53	4.16
20	(6)	0.77	0.86	1.01	1.39	1.73	3.16	4.98
26	(60)	0.12	0.25	0.35	0.63	0.90	1.84	3.30
29	(100)	...	0.06	0.17	0.46	0.72	1.35	2.82
Aug. 1	(28)	0.20	0.22	0.27	0.57	0.85	1.65	3.12
8	(33)	0.17	0.21	0.39	0.60	1.05	2.01	2.97
12	(22)	0.24	0.29	0.48	0.85	1.21	2.24	3.99
17	(30)	0.19	0.27	0.41	0.71	1.08	1.89	3.47
22	(100)	...	0.11	0.16	0.51	0.75	1.32	2.88
24	(16)	0.32	0.42	0.59	0.89	1.28	2.01	3.34
29	(100)	...	0.08	0.21	0.54	0.93	1.77	3.21
Sept. 2	(18)	0.30	0.42	0.47	0.88	1.14	1.82	3.44
7	(24)	0.22	0.31	0.39	0.77	1.30	2.81	3.40
12	(70)	...	0.13	0.31	0.49	0.86	1.46	3.18
20	11	0.51	0.64	0.67	0.98	1.36	1.97	3.46
22	5	0.96	1.11	1.36	1.80	2.18	2.90	4.50
24	8	0.62	0.75	0.99	1.20	1.53	2.21	3.78
28	15	0.42	0.50	0.65	0.91	1.21	1.91	3.55
Nov. 17	56	0.07	0.15	0.20	0.38	0.63	1.24	2.84
22	(0.6)	8.1	8.5	8.9	9.3	9.9	10.3	...
24	(0.4)	11.0	11.3	11.5	11.6	12.1	...	...

hydrogen-arc systems were reduced to atmospheric attenuation coefficients by conventional photographic spectrophotometry. A Knorr-Albers microphotometer was modified to cover a range of three density units. Corrections were applied for photographic fogging due to light scattered inside the spectrograph, for differences in the astigmatic heights of long- and short-path spectra, and for the small dissimilarity in spectral reflectances of the mirrors in the xenon-arc system. This last correction was derived by comparing attenuation data yielded by the hydrogen-arc system with uncorrected data yielded by the xenon-arc system.

Stray light from extraneous sources was found to be entirely negligible for the 10-second exposures. For 1000-second exposures with the hydrogen-arc system in Pasadena, faint fogging due to street lights began to appear; the maximum resulting density was approximately 0.08, for which a correction could be easily applied. In Washington, stray light was successfully eliminated by baffles.

RESULTS

Ultraviolet attenuation coefficients were plotted against wavelength for 78 representative nights among 125 nights on which spectra were photographed at Pasadena and also for three nights on which similar spectra were obtained at Washington, D. C. The Pasadena results are summarized in Table I. The coefficients for each night are tabulated at seven wavelengths: 4300, 4000, 3600, 3200, 2900, 2620, and 2400 angstroms. The visibility ranges were either measured with the Loofah haze-meter or extrapolated (indicated by parenthesis) from the attenuation curve. It will be noted that the first 45 nights in the table are consecutive.

In Fig. 5, the attenuation curves for six representative nights in Pasadena show a little more detail than Table I. They illustrate typical shapes and features. Over most of the spectral region plotted, the absolute values of σ are correct to 0.05 or less, and the relative accuracy of neighboring points should be somewhat better than that. Errors in wavelength measurement are negligible.

It is evident from Fig. 5 that two curves can have equal or nearly equal values of σ at one wavelength but be quite different at another. This behavior is further illustrated by Fig. 6, which is a typical group

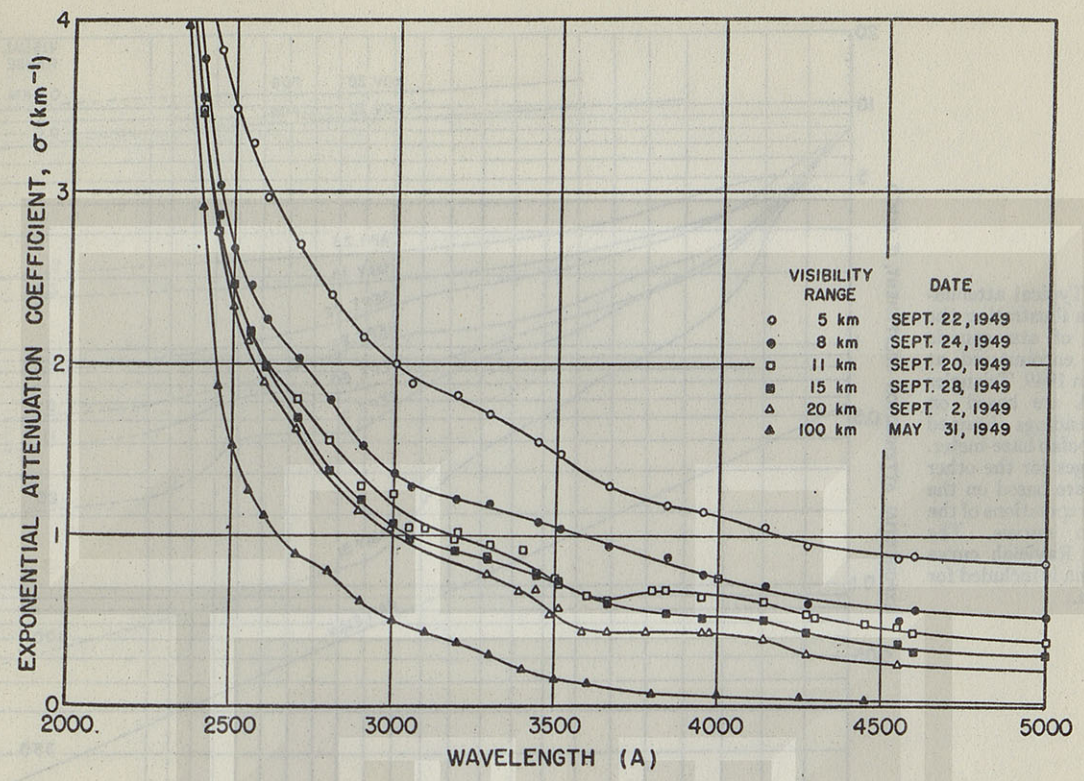

FIG. 5. Spectral attenuation curves for six nights at Pasadena illustrating typical shapes and features. Note that two curves having equal attenuation coefficients at one wavelength can be quite different at another.

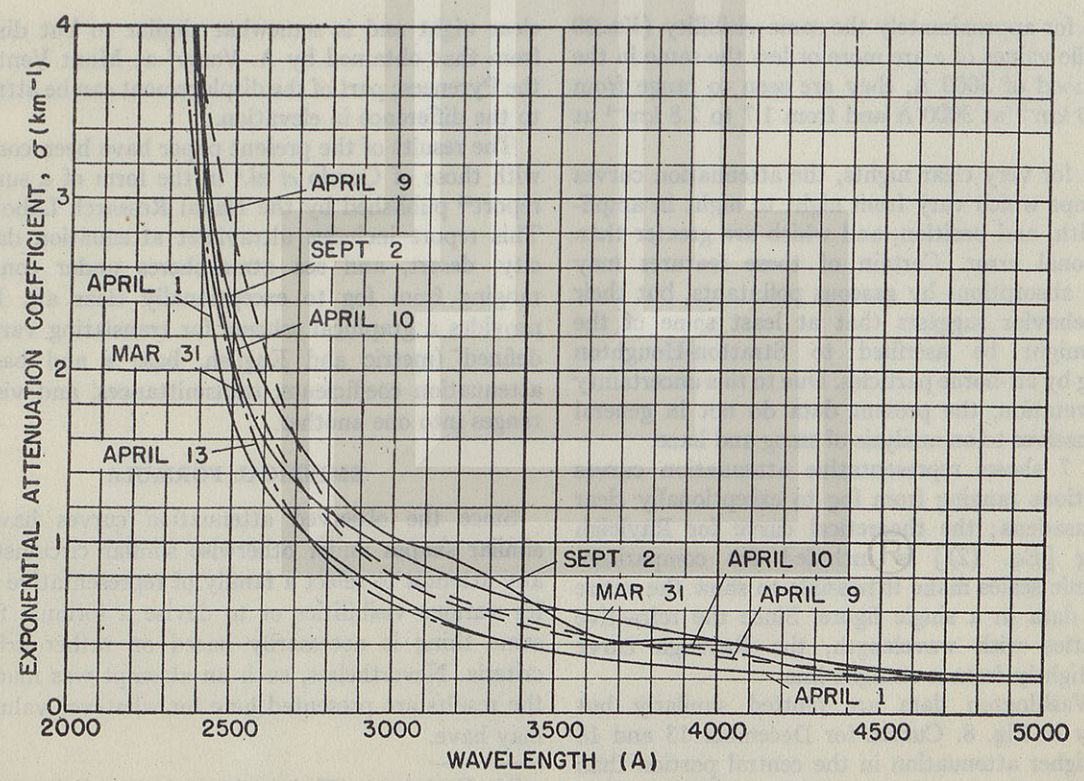

FIG. 6. A selected group of attenuation curves for approximately the same visibility ($V \simeq 20$ km) showing how they tend to diverge in the ultraviolet. All were obtained at Pasadena in 1949.

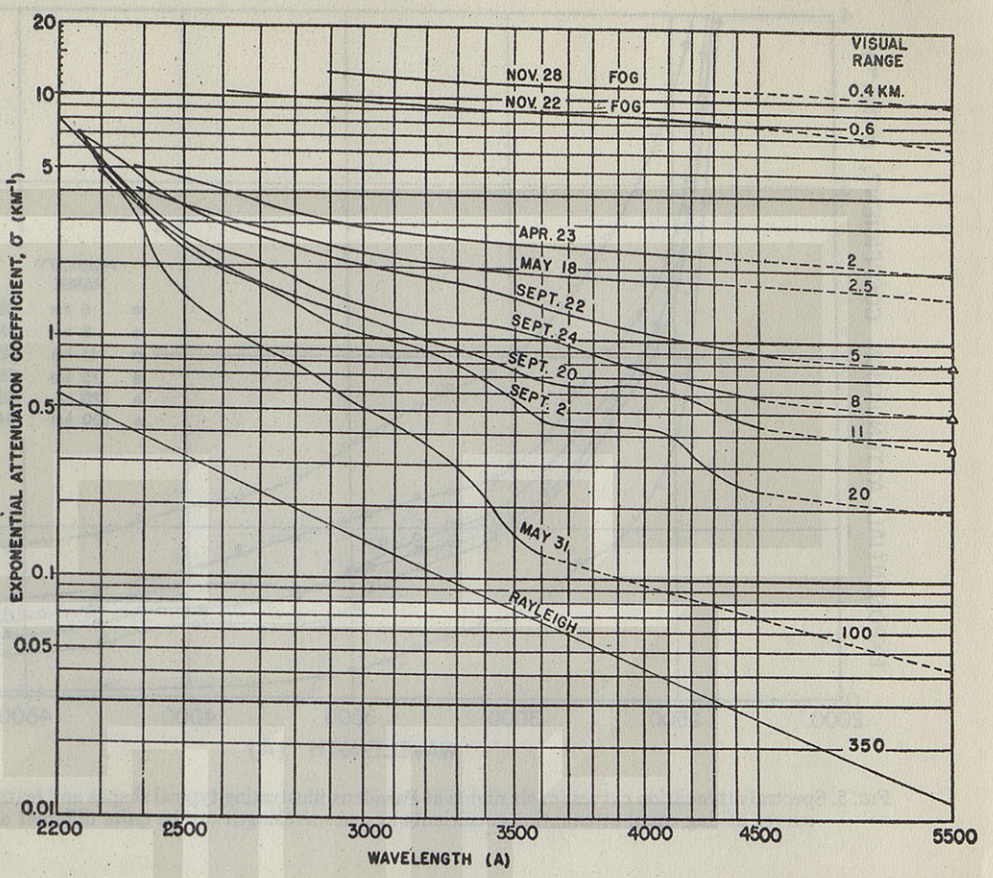

FIG. 7. Typical attenuation curves illustrating the full range of atmospheric conditions encountered at Pasadena in 1949. Triangles at 5500 A are based on visibility readings obtained with the Loofah haze-meter. Visual ranges for the other six nights are based on the dashed extrapolations of the attenuation curves. The theoretical Rayleigh curve for Pasadena is included for comparison.

of curves for approximately the same visibility ($V \simeq 20$ km). While values of σ are more or less the same in the neighborhood of 5000 A, they are seen to range from 0.6 to 1.0 km^{-1} at 3000 A and from 1.7 to 2.8 km^{-1} at 2500 A.

Except for very clear nights, the attenuation curves have humps which vary from night to night in amplitude, width, and position, and which are greater than observational error. Certain of these features may represent absorptions by gaseous pollutants, but their erratic behavior suggests that at least some of the humps might be ascribed to Stratton-Houghton scattering by air-borne particles. Due to this uncertainty of interpretation, the present data do not in general lend themselves to an analysis of smog and haze.

Figure 7 shows representative attenuation curves for conditions ranging from fog to exceptionally clear air at Pasadena; the theoretical curve for Rayleigh scattering [Eq. (2)] is included for comparison. Logarithmic scales make it possible to show the entire range of data in a single figure. Since the refractive index varies with wavelength, the Rayleigh curve departs slightly from a straight line.

The Washington data are plotted similarly but separately in Fig. 8. Curves for December 13 and 18 show a higher attenuation in the central portion than do most Pasadena curves for similar visibilities. The curve for November 6 was obtained during a relatively clear night and is somewhat similar to but displaced from that obtained by A. Vassy[7] at Mont Ventoux in the Pyrenees; part of the displacement can be attributed to the difference in elevation.

The results of the present paper have been combined with those of Curcio *et al.*[5] in the form of a summary report[50] published by the Naval Research Laboratory. This report includes ultraviolet attenuation data for city, desert, and sea atmospheres under conditions ranging from fog to exceptionally clear air. It also provides a graphical scheme for translating variously-defined (metric and English, base e and base 10) attenuation coefficients, transmittances, and visibility ranges into one another.

EMPIRICAL FORMULA

Since the observed attenuation curves have dissimilar shapes under otherwise similar circumstances, any attempt to select a family of representative curves for various visibilities or to devise a formula for the same thing is necessarily based on rather arbitrary criteria. Nevertheless, such an attempt was made and the results are presented here for whatever value they may have.

[50] L. Dunkelman, "Horizontal attenuation of ultraviolet and visible light by the lower atmosphere," Naval Research Laboratory Report 4031, September 1952.

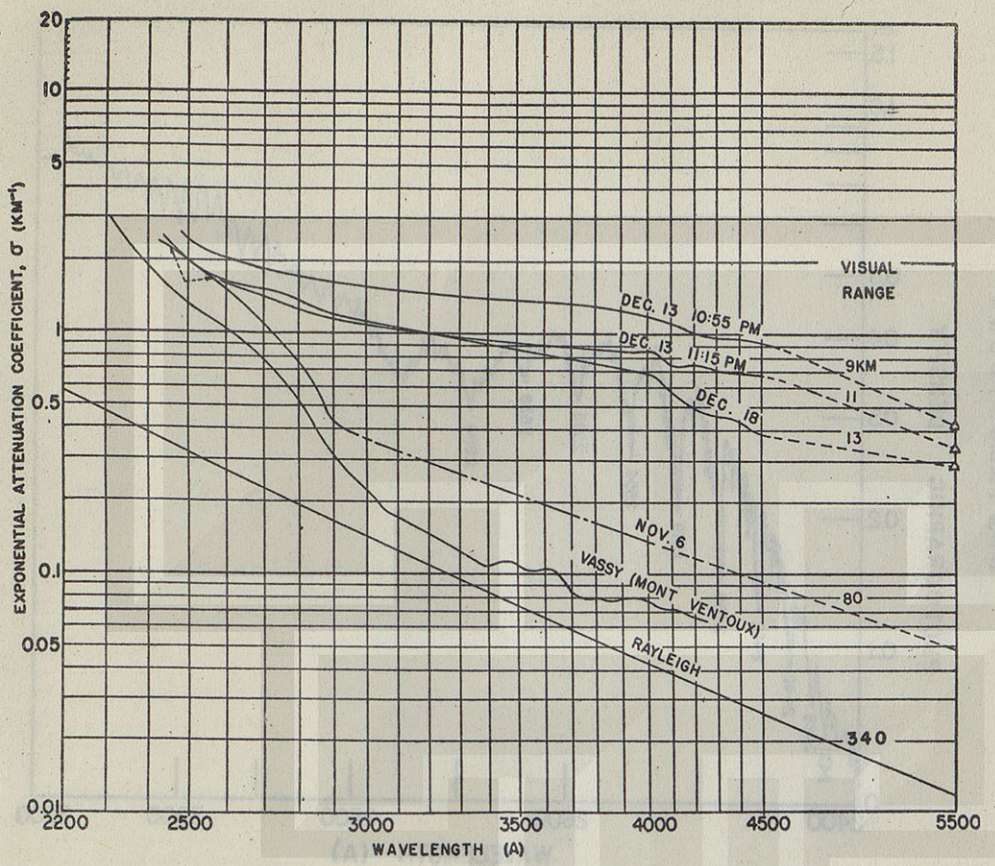

FIG. 8. Spectral attenuation curves obtained with the hydrogen-arc system at Washington in 1950. Triangles and visual ranges have the same basis as in Fig. 7. The maximum scatter of points from the curves was ± 0.02 km^{-1}. The detection of ozone and sulfur dioxide at Washington is discussed in the text. Vassy's curve for exceptionally clear air at Mont Ventoux and the theoretical Rayleigh curve for Washington are included for comparison.

The first step toward selecting a representative family of attenuation curves was to examine the correlation between the values of σ at various wavelengths. When σ for each of the wavelengths in Table I was plotted as ordinate against $\bar{\sigma}$ for 5500 A as abscissa, a scatter of points was obtained, one point for each spectrogram analyzed. This scatter tended to have a lower boundary, and an envelope drawn along it was found to pass through or near points associated with nights when the air was believed to be comparatively free of pollutants. In the main, points lying substantially above the envelope represented somewhat smoggy conditions or at least stagnant city air, implying that smog tends to introduce more pronounced attenuation in the ultraviolet than in the visible region. Two or three isolated nights whose points fell substantially below the envelope represented conditions when the air was filled with abnormally large particles, such as rain or falling mist; as one might expect, such an atmosphere tends to be spectrally more neutral than average. In general, however, it is not practicable to try correlating attenuation coefficients with the usual meteorological variables.

In each $(\sigma,\bar{\sigma})$ plot, the envelope associated with unpolluted air could be approximated by

$$\sigma = m\bar{\sigma} + \sigma_0 \qquad (4)$$

in the range $0.1 < \bar{\sigma} < 1.0$. Using the observed dependence of the slope m and the intercept σ_0 on wavelength, and translating $\bar{\sigma}$ into visibility range V by means of Eq. (3a), one obtains

$$\sigma = \frac{5380-\lambda}{280V} + \left(\frac{800}{\lambda-1800}\right)^3, \qquad (4a)$$

where λ is in angstroms, V in km, and σ in km^{-1}. It must be emphasized that formula (4a) is a totally empirical result associated with no particular physical interpretation. It represents an approximate lower bound on the exponential attenuation coefficient σ for $4 < V < 40$ and for $2400 < \lambda < 4000$.

GAS ABSORPTION

The Ciechomski oxygen bands[33,34] were found on all 128 nights on which transmission spectra were photographed. The only other observed band system was that due to sulfur dioxide[51] found on two nights at Washington. Neither of these two weak-band systems is shown in any of the (σ,λ) curves, but both can be seen on the microphotometer tracing in Fig. 9. Except for these bands, the ultraviolet attenuation coefficient was found to be a smooth, though often wavy, function of wavelength down to 2300 A, indicating that coefficients determined with an emission-line source[1–5] should be at least roughly correct over most of that region. The

[51] J. H. Clements, Phys. Rev. 47, 224 (1935).

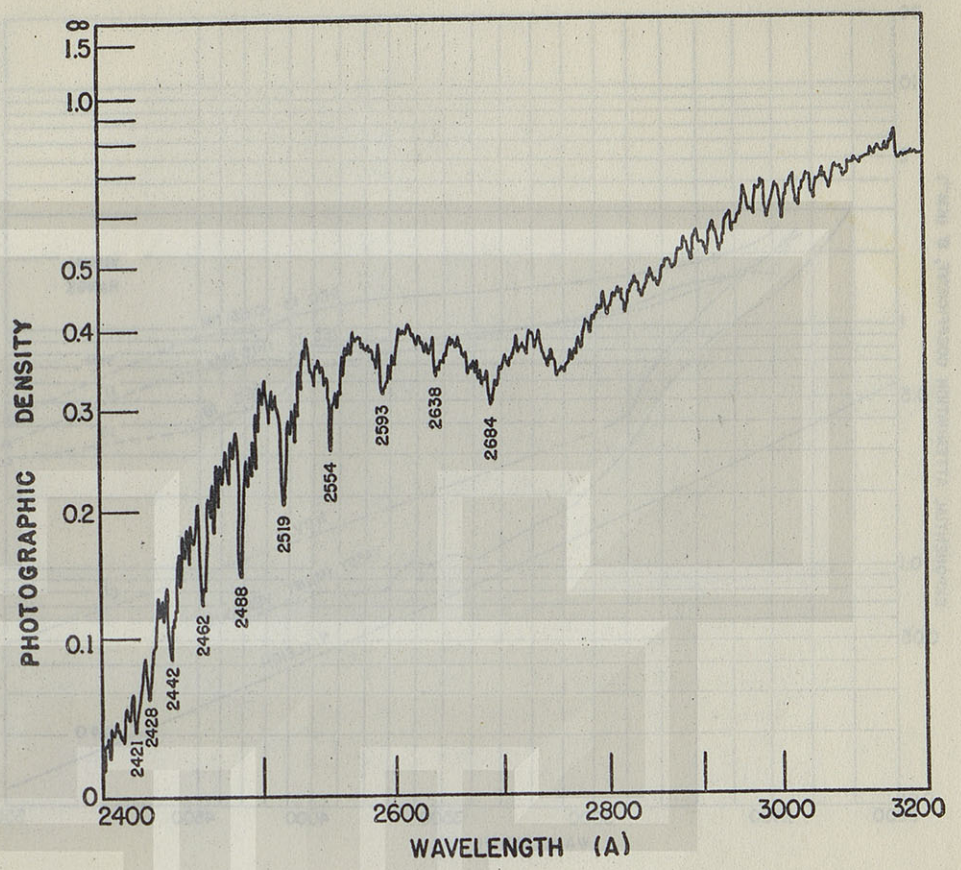

FIG. 9. Microphotometer tracing of part of the hydrogen-arc spectrum photographed over a path length of 0.9 km at Washington on December 18, 1950. Wavelengths of the heads of the Ciechomski oxygen bands are labeled along the tracing. The many faint dips in the tracing between 2800 A and 3150 A are weak sulfur-dioxide bands.

importance of validating emission-line results has already been emphasized in the Introduction.

In Fig. 8, the attenuation curve for Washington on November 6 and Vassy's[7] curve for Mont Ventoux appear to have somewhat similar ozone humps. By use of Fabry and Buisson's method,[25] together with the ozone absorption coefficients of Ny and Choong,[30] the concentration of ozone at Washington on November 6 was estimated to be about 3 parts per 100 million. Vassy's estimate for Mont Ventoux was 2.5 parts per 100 million. These values are in the same general range also found by others.[25–31] Except under very clear conditions it was impossible to estimate ozone concentrations from the σ,λ curves, because the irregular spectral attenuation due to haze buried any small contribution which may have been due to ozone.

When sulfur dioxide was detected on December 13 and 18, the attenuation curves did not suggest ozone (see Fig. 8); whereas on November 6 when ozone was apparently present, the spectra showed no trace of sulfur dioxide. This is in keeping with Glueckauf's statement[52] that air tends to be free of sulfur dioxide in the presence of ozone. By comparison with the absorption of laboratory samples, the concentration of sulfur dioxide at Washington on December 13 and 18 was estimated to be about 8 parts per 100 million.

ACKNOWLEDGMENTS

The advice of Dr. Richard Tousey at the Naval Research Laboratory materially aided the progress of this investigation. Thanks are due Dr. Oliver R. Wulf of the United States Weather Bureau for the use of his quartz objective spectrograph. The assistance of Robert C. Serviss of the California Institute of Technology and Elio V. Serra of the Naval Research Laboratory was appreciated.

[52] E. Glueckauf, *Compendium of Meteorology*, T. F. Malone, ed. (American Meteorological Society, Boston, 1951), p. 7.

NRL REPORT 4031

C

HORIZONTAL ATTENUATION OF ULTRAVIOLET AND VISIBLE LIGHT BY THE LOWER ATMOSPHERE

Lawrence Dunkelman

Micron Waves Branch
Optics Division

September 10, 1952

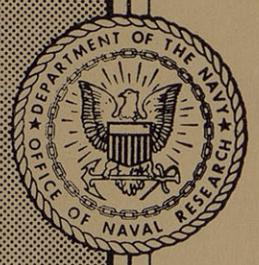

NAVAL RESEARCH LABORATORY

WASHINGTON, D.C.

ABSTRACT

The horizontal attenuation of ultraviolet and visible light by the lower atmosphere has been measured at night in city, desert, and sea atmospheres under conditions ranging from fog to exceptionally clear air. The researches are summarized and the data are presented in the form of representative spectral attenuation curves for all the locations investigated and in tables of spectral attenuation coefficients for the locations where sufficient data were obtained to warrant their preparation, for various visibilities, as follows: (a) Pasadena, California, from 2400 A to 6000 A for visibility, V, from 3.9 to 39 km; (b) Chesapeake Bay, Maryland, combined with Dry Tortugas, Florida, from 2970 A to 5780 A for V from 9.8 to 78 km; (c) Marshall Islands, Pacific Ocean, from 3020 A to 5780 A for V from 15.5 to 78 km. The tables are intended for those who require a survey of typical spectral attenuation characteristics of the lower atmosphere. For those requiring accurate coefficients for a given time and place, there are given references to methods for making the required measurements. A diagram is given for converting between the attenuation coefficients, σ(base e) and σ_{10} (base 10), and transmittance t, per sea mile and per kilometer. Cautions in selection and use of tables are given and the effects of field of view and of gaseous absorption are discussed.

The data which have been collected permit the following conclusions: (a) several different types of attenuation function are found in a city atmosphere unlike those found over the sea or in the desert, whereas attenuation curves at stations outside cities appeared to follow a particular pattern at each location; (b) for similar visibilities the city data show a higher attenuation in the middle ultraviolet than do the data taken outside cities. (c) the spectral attenuation curves for a Nevada desert are characterized by their proximity to Rayleigh scattering; (d) it was difficult to determine the composition of smogs when they were encountered, but, under some conditions, it was possible to detect sulphur dioxide and to make approximate measurements of its concentration. Under clear weather conditions it was possible to detect ozone when it was present in the lower atmosphere and also to make approximate measurements of its concentration.

PROBLEM STATUS

The data presented herein are the results of investigations by the Radiometry I, Radiometry II, and Micron Waves Branches. This report concludes the work on this phase of the problem; work continues on the basic problem.

AUTHORIZATION

NRL Problem NO3-14
RDB Projects NR 473-140 and NE 120-713-T-2

Manuscript submitted July 22, 1952

CONTENTS

HORIZONTAL ATTENUATION OF ULTRAVIOLET AND VISIBLE LIGHT BY THE LOWER ATMOSPHERE

INTRODUCTION

The attenuation of light at night over a horizontal path in the lower atmosphere has been the subject of two recent investigations at the Naval Research Laboratory. During 1948-1950, Baum and Dunkelman (1) measured atmospheric attenuation from the blue portion of the spectrum to 2300 Angstroms in the ultraviolet. The work was conducted at Pasadena, California and at Washington, D. C. by employing an objective prism spectrograph to photograph a source with a continuous spectrum over a suitable light path. During 1949-1951 Stewart et al.(2) made similar measurements in the near ultraviolet and visible spectrum on the Chesapeake Bay, Maryland; at Dry Tortugas, Florida; Washington, D. C.; the Marshall Islands; and at an elevation of 4500 feet in Nevada. They employed a pair of slit spectrographs and photographed a source having line spectra. The purpose of this report is to summarize and compare the results of these measurements.

At the start it was thought that the entire spectral attenuation curve of the atmosphere would be found to depend on a single parameter such as the visibility. This assumed that atmospheric spectral attenuation curves would coincide approximately at all wavelengths if they coincided at one wavelength. Put in another way, the assumption asserted that all optical properties of all hazes are approximately the same if any single optical property is the same. The experimental results did not support this hypothesis; it has not been possible to fit all the experimental data into a single family of curves. However, several types of atmosphere have been arbitrarily separated, and the data for each of these are presented in the form of tables of spectral attenuation.

There were expectations that there might be a simple correlation between spectral attenuation functions and certain meteorological variables such as relative humidity, and that analysis of the curves might throw light on the aerosol content, the industrial pollutants (smog), and the concentration of ground ozone. However, no correlation with relative humidity was found; it was not possible to determine the size distribution of haze particles; and it was difficult to judge the composition of the smogs when they were encountered. Under certain conditions, nevertheless, it was possible to detect sulphur dioxide and to make approximate measurements of its concentration. Under clear weather conditions it was possible to detect ozone when it was present in the lower atmosphere and also to make approximate measurements of its concentration.

The Pasadena atmosphere was investigated on many nights over a period of one year, and a large range of visibilities was covered. Several different types of attenuation function were encountered, and they were unlike those found over the sea or in the desert. At the stations outside cities and industrial areas, the attenuation curves found over the relatively short periods of the investigations appeared to follow a particular pattern at each location.

For the solution of problems requiring a knowledge of atmospheric attenuation there are, therefore, two avenues of approach. If accurate attenuation coefficients are needed for a given time and place, it is necessary to make the measurements then and there. Several methods exist for accomplishing this (see References 1 and 2 and their bibliographies). If on the other hand, a survey of the attenuation characteristics of the atmosphere in a certain wavelength band is sufficient, the results herein should provide valuable guidance.

RELATED TOPICS

Visibility

The most convenient and obvious characteristic of the atmosphere relating to the attenuation is the horizontal visibility range, V, frequently referred to as the "daylight visual range," the "visual range" or simply the "visibility." V is defined to be the distance at which one can see a large black object in daylight against the sky near the horizon. The international visibility code describing certain conditions of atmospheric clarity is given in Table 1. For reference, corresponding attenuation coefficients have been included.

TABLE 1
International Visibility Code

Code No.	Description	Daylight Visual Range (metric)		Exponential Attenuation Coefficient (km^{-1})	
		From	To	From	To
0	Dense fog		< 50 m		> 86
1	Thick fog	50 m	200 m	86	21
2	Moderate fog	200 m	500 m	21	8.5
3	Light fog	500 m	1 km	8.5	4.3
4	Thin fog	1 km	2 km	4.3	2.1
5	Haze	2 km	4 km	2.1	1.1
6	Light haze	4 km	10 km	1.1	0.43
7	Clear	10 km	20 km	0.43	0.21
8	Very clear	20 km	50 km	0.21	0.07
9	Exceptionally clear	> 50 km		< 0.07	

Spectral Attenuation of Light

A collimated beam of light, passing through air, is attenuated both by scattering and by absorption. The spectral attenuation coefficient, σ, is defined by

$$i = i_0 e^{-\sigma x} \qquad (1)$$

where i and i_0 are the intensities at wavelength, λ, entering and emerging respectively, from a column of the atmosphere x km in length. σ comprises both scattering by haze particles and air molecules, and absorption by air and the impurities in it. In the case of air near the earth's surface, several factors contribute to attenuation, and the total coefficient is the sum of the coefficients for the individual contributors. Thus, we may write

$$\sigma = \sigma_A + \sigma_B + \sigma_C \qquad (2)$$

where:

σ_A is the component due to Rayleigh scattering by air molecules,

σ_B represents scattering and true absorption by water droplets and airborne particles,

σ_C is due to absorption by gases.

Relation Between Visibility and the Attenuation Coefficient

The relation between the horizontal visibility and the attenuation coefficient, given originally by Koschmieder and described by Hulburt (3) and Middleton (4), is

$$V\bar{\sigma} = \ln\frac{1}{\eta} \qquad (3)$$

where η = the threshold value of brightness contrast of the eye. Since this expression deals with vision, $\bar{\sigma}$ is the average attenuation coefficient for daylight as seen by the human eye. Numerically, $\bar{\sigma}$ is approximately equal to the spectral attenuation coefficient σ at about 5500 A. For daylight and large black objects it is customary to take $\eta = 0.02$, hence Equation (3) becomes:

$$V\bar{\sigma} = 3.92. \qquad (3a)$$

Alternative Quantities Used in Describing Atmospheric Attenuation

In the present report the exponential attenuation coefficient, σ, as defined by Equation (1), is used to describe the atmosphere. There are, however, several alternative coefficients which are often preferred, and which are simply related to σ:

(a) Decimal attenuation coefficient, σ_{10} per kilometer defined by $i = i_o\, 10^{-\sigma_{10} x}$. σ and σ_{10} are related by $\sigma_{10} = 0.4343\sigma$. σ_{10} is identical with the optical density per kilometer.

(b) Transmittance per kilometer defined by

$$t = \frac{i}{i_o} = e^{-\sigma} = 10^{-\sigma_{10}}. \qquad (4)$$

Those who visualize the atmosphere as an optical filter usually prefer to characterize it by giving t, the transmittance per kilometer. On the other hand, those more accustomed to electrical and acoustical work prefer to use (-log t), which is the optical density per kilometer and is also σ_{10}, since this is a logarithmic unit having properties similar to the decibel. In fact, the light intensity loss in decibels per km is 10 times the optical density per km.

It is sometimes convenient to describe the attenuation by a range, R km, at which the light intensity, i, is reduced to a certain fraction, 1/K, of its initial value i_o. In general,

from Equation (1)

$$R = \frac{1}{\sigma} \ln K = \frac{1}{\sigma_{10}} \log K. \quad (5)$$

Thus, the ranges at which i_o is reduced to $1/e\ i_o$ and $1/10\ i_o$ are $1/\sigma$ and $1/\sigma_{10}$, respectively. The range required for a reduction to $1/100\ i_o$, is $2/\sigma_{10}$, etc.

Conversion Diagram

In order to simplify conversion from one quantity to another, Plate A* was prepared. This diagram represents graphically the relation between the visibility, V, the various attenuation coefficients, and the transmittance of the atmosphere. The following conversions can be made:

(a) conversion of any one of V, σ, σ_{10}, or t into any of the others; e.g., σ into t;

(b) conversion of V, σ, σ_{10}, or t from its value in terms of kilometers into its value in terms of sea miles, (sm) or vice versa; e.g., t (per km) into t (per sm).

(c) conversion of one quantity in one length unit into another quantity in the other length unit: e.g., V (in km) into t (per sm).

SPECTRAL ATTENUATION OF THE ATMOSPHERE

Curves of Attenuation

Representative attenuation curves obtained at the several geographical locations are presented in Plate B and Figures 1 and 2. The attenuation coefficient σ, is plotted against the wavelength. Logarithmic scales are used since this causes the "Rayleigh" curve for molecular scattering, $\sigma \propto \lambda^{-4}$, to be a straight line, except for a small departure due to dispersion. Logarithmic scales also make it possible to show the entire range of data on a single sheet of paper with reasonable accuracy. The spectral region covered by the Pasadena and Washington measurements of Baum and Dunkelman (1) was approximately 2300 A to 4400 A; the measurements by Stewart et al.(2) lay within the region from 2650 A to 5780 A, the exact range depending on the path lengths used at the various geographical locations.

The experimental error in σ depended largely on the distance over which the measurements were made. For Pasadena and Washington the probable errors in σ were estimated to be $\pm 0.05\ km^{-1}$ and $\pm 0.02\ km^{-1}$ respectively. For other locations (excepting Mont Ventoux (5)) the error was of the order of $\pm 0.01\ km^{-1}$.

The approximate visual range, V, is given for each curve. This makes it possible for one to associate a particular curve with a characteristic of the atmosphere that is probably familiar to him. Since all measurements described in this report were made at night, V could not be measured by direct visual observation. In the case of the Pasadena experiment, the value of V on some of the nights was determined using Equation (3a) from measurements of $\bar{\sigma}$ made with the British Admiralty Hazemeter known as the "Loofah" (6). The Loofah data are shown on the curves by the triangle points plotted at λ 5500 A. The broken lines connecting the spectral curve with the points obtained from Loofah serve only to

*Plate A is on the same page as Plate B and is so arranged that it can be used directly with the curves of Plate B which are discussed in the next chapter. Also, when this page is unfolded, the diagram is convenient to use with any of the other curves and tables in this report. Instructions for use are given on the diagram.

identify the points and do not represent experimental values for the interval 4400-5500 A. When Loofah was not available, the curves were extrapolated from the blue region to 5500 A and this value of $\overline{\sigma}$ was checked insofar as possible against the best estimates that could be made from afternoon observations of visibility and atmospheric stability.

In other geographical regions, the measurements included σ_{5460A} which was taken as $\overline{\sigma}$, and from Equation (3a) gave V. During the Chesapeake Bay, Dry Tortugas, and Nevada experiments, a visual telephotometer (7) was used in addition, and $\overline{\sigma}$ obtained from this instrument agreed with σ_{5460A} obtained by the spectrophotographic method.

The curves shown in Plate B were selected to include at least one obtained at each geographical region and to include a spread of atmospheres covering visual ranges from 0.4 to 100 km, the foggiest and clearest atmospheres measured. Many other σ vs. λ curves were obtained and additional data are given in References 1 and 2. The Rayleigh atmosphere shown by the straight line corresponds to a visual range of 330 km. This ideal pure atmosphere in effect sets the upper limit to the transparency of the lower atmosphere at sea level and is useful for comparison.

Pasadena, California – The Pasadena data, taken over a period of one year and including 125 nights of which 80 were consecutive, permit making a study of the changes taking place in the attenuation function at one locality from night to night. It was found that the curves sometimes cris-crossed and disagreed in the ultraviolet for nights of approximately the same visual range. Figure 3* is a typical grouping of curves for V = 20 km and illustrates at 3000 A, for example, that σ ranges from 0.6 to 1.0 km^{-1}. The curves for this and also for other visibilities show humps which vary from night to night in amplitude, width, and position, and which are outside experimental error. Since they were not associated with discrete absorption lines or bands, and were erratic in behavior, they were not attributed to absorption by a gaseous pollutant. It is tempting to ascribe these humps to Stratton-Houghon scattering by airborne particles of fairly uniform size but we have no proof. This would require a detailed and simultaneous study of the aerosol, similar to those made by Dessens (8) who captured the particles on spider webs.

The topographic features of the Pasadena-Los Angeles area are frequently a factor in accentuating pollution of the air caused by stagnant anticyclonic conditions which may persist for several days. It is difficult to judge how typical a polluted or industrial atmosphere one finds in Pasadena, for we have not carried out measurements in other industrial regions. It is likely that different industrial areas have different types of haze. It also seems probable that the variations that occur in the type of haze from day to day or week to week depend on topographic features, winds, and nature of industrial activity.

Randle Cliff on the Chesapeake Bay, Maryland – Two curves for Randle Cliff on the Chesapeake Bay, Maryland are shown on Plate B. Their shape is typical of the curves for nine nights of measurements made there during February to April 1950 and described in detail in Reference 2. For similar visibilities the Pasadena data show a higher attenuation in the middle ultraviolet. The atmosphere is clear or very clear at this location, which is in a region of farms and is relatively free from heavy industry. While the air may occasionally be somewhat polluted by smoke from Baltimore, 40 miles to the north, it is much more often clean than smoggy. Pearson et al.(7) made many visual measurements of atmospheric transmittance at night at this location over a two-year period and found the transmittance to be 0.9 per kilometer or greater for more than half of the nights.

Dry Tortugas, Florida – The measurements of atmospheric attenuation at Dry Tortugas were made during five nights in May 1950 and the results were nearly the same night after night. One representative curve is given in Plate B and shows that the atmospheres at Randle Cliff on the Chesapeake Bay and Dry Tortugas are similar.

*For this figure a linear plot was found to be more suitable than a logarithmic plot.

Marshall Islands, Pacific Ocean – During March and April 1951, observations were made on five nights at one location in the Marshall Islands. The measurements were made over a path 1500 ft down wind from a breaking surf. Two of the curves obtained (Plate B) are typical and characterized by their relative flatness. It is probable that the nearly neutral attenuation was due to scattering by large particles originating from sea spray.

A Desert, Nevada – The atmospheric attenuation was investigated during five nights in a desert region at a 4500-foot elevation in Nevada and two of the curves are shown in Figure 1. All Nevada curves were characterized by their proximity to the Rayleigh scattering curve for a 4500-foot elevation, which is also given in Figure 1.

Washington, D. C. – Attenuation measurements were made in Washington, D. C., on three nights in the Fall of 1950 and the results are shown in Figure 2 and Plate B. The December 13 and 18 curves show a lower attenuation in the middle ultraviolet than do the Pasadena curves for similar visibilities. The November 6 curve on Plate B was obtained during an exceptionally clear night and is rather similar to that obtained by A. Vassy (5) at Mont Ventoux in the Pyrenees, though the air was not quite as clear.

Comparison of Continuous and Line Source Systems

One of the objects of the experiments at Washington was to compare directly the methods employing continuous and line sources described in References 1 and 2 respectively. It was expected that the results would be in agreement unless it happened that certain of the wavelengths used in the line spectrum method coincided with discrete absorption lines due to some gaseous component of the atmosphere. It was possible to make the comparison only on the night of December 13, 1950; the atmosphere was rather hazy (4 km visibility) and was unstable, affording poor conditions for the work. The results are shown in Figure 2. The curve is the mean result of two determinations extending from 1040 to 1110 PM using the continuous spectrum method. The points are the average of three determinations made from 1020 to 1150 PM using the line source method; the source was a mercury arc. The agreement of results is reasonable. It is likely that difficulties in averaging over a period of varying atmospheric haziness caused the discrepancies in σ to be somewhat greater than the probable error of ± 0.02 km^{-1} for the path length used.

It was concluded that the use of a mercury arc source is permissible and does not produce errors due to discrete absorption effects. If other line sources are used, care must be taken to avoid the Herzberg absorption bands of O_2 lying between 2421 A and 2684 A, and possibly the bands of SO_2 if this pollutant is present in great concentration. We have concluded therefore, that one should employ a continuous source when required spectral attenuation data fall within the region of discrete absorption of O_2 or within spectral regions having discrete absorption due to gaseous pollutants whose presence is known or suspected.

Effects of Gaseous Absorption

In addition to attenuation by scattering, absorption by oxygen, and ozone if present, causes the attenuation curve to rise even more rapidly at wavelengths below about 3100 A; i.e., in Equation (2) σ_C becomes important. These effects combine to set an upper limit to the transparency of air in this spectral region.

Ozone is known to exist as a variable constituent in the lower atmosphere in concentrations from 0 to 0.07 parts per million (ppm). Stated in another way, the amount of ozone in reduced thickness at STP ranges from 0.0 to 0.07 mm per kilometer of air. Within this range of concentration, ozone absorbs appreciably from about 3100 to 2000 A; at its peak absorption, 2550 A, σ is 2.25 km^{-1} for 0.07 mm ozone per km. Table 2 presents the absorption coefficients of ozone, and σ_C values for an average and a high value of ozone concentration, 0.02 and 0.07 mm/km respectively.

In case there is haze present, the atmospheric attenuation curve from the visible down to 3100 A lies well above the Rayleigh curve and optical determination of ozone becomes difficult or impossible. To determine the absorption by the ozone alone it is necessary to subtract from the measured total attenuation in the region below 3100 A where ozone absorbs the portion due to scattering. This can be done only by extrapolating below 3100 A, in some arbitrary fashion, the measured curve above 3100 A. This process is not possible in general because the attenuation curve due to scattering does not follow any simple law.

TABLE 2
Ozone Absorption in the Lower Atmosphere

Wavelength (A)	Exponential Absorption Coefficient per cm (STP) of O_3*	$\sigma(km^{-1})$ per km for 0.02 ppm of O_3	$\sigma(km^{-1})$ per km for 0.07 ppm of O_3
3200	0.92	0.0018	0.0064
3100	2.99	0.0060	0.021
3000	11.5	0.023	0.081
2900	46	0.092	0.32
2800	127	0.25	0.89
2700	230	0.46	1.61
2600	322	0.64	2.25
2500	322	0.64	2.25
2400	230	0.46	1.61
2300	134	0.27	0.94
2200	51.6	0.12	0.40
2100	23.0	0.046	0.16

*Ny Tsi-Ze and Choong Shin-Piaw, Chinese J. Phys., 1, 1 (1933)

Absorption by oxygen itself commencing and increasing rapidly below 2500 A as a continuum must also be considered. In Table 3 are presented the absorption coefficients of oxygen and the values of $\sigma(km^{-1})$ of pure air due to oxygen absorption. The curve of attenuation for Rayleigh scattering plus oxygen absorption is shown in Figure 4 as curve A. Curve B presents the attenuation of pure air having ozone in a concentration of 0.02 ppm; this is obtained by adding to curve A the absorption values given in the third column of Table 2. Curve C includes ozone present in a concentration of 0.07 ppm obtained similarly from the fourth column of Table 2.

Discrete but weak absorption by oxygen also occurs in the Herzberg bands between 2649 and 2421 A. These bands appeared in the spectra photographed over an air path of 0.68 km using a continuous source, and are reproduced in Reference 1. They are not included in any of the attenuation curves because of their relative unimportance. However, they can not be neglected in cases where attenuation coefficients at certain wavelengths coinciding with those of discrete oxygen absorption, are needed. Such a situation would require further quantitative investigations over specified path lengths in the appropriate wavelength interval.

Nitrogen, the other principal component of air, does not begin to absorb until well into the vacuum ultraviolet and attenuates only through Rayleigh scattering in visible and ultraviolet.

Sulphur dioxide is a gas which at times exists as a pollutant in the atmosphere and absorbs in the ultraviolet. The absorption bands in the region 3200 to 2750 A are rather closely spaced and become diffuse below 2750 A. In the concentrations known to exist in polluted atmospheres, less than one part per million, the absorption is weak.

TABLE 3
O_2 Absorption

Wavelength (A)	Exponential Absorption Coefficient per cm (STP) of O_2*	σ (km^{-1}) per km of Pure Air Due to O_2 Absorption
2600	5.1×10^{-6}	0.11
2500	1.8×10^{-5}	0.36
2400	5.8×10^{-5}	1.16
2300	1.29×10^{-4}	2.58
2200	2.16×10^{-4}	4.32
2100	4.14×10^{-4}	8.28

*Compilation from the data of Buisson, Vassy, Götz, and Granath.

Returning now to the curves of Plate B, we see that the Mont Ventoux curve and the Washington curve for November 6, each has a shape resembling the curve for 0.02 ppm of ozone in Figure 4. By selecting an ozone concentration such that the best match to the experimental curve was obtained, we found 0.03 ppm in Washington whereas Vassy found 0.025 ppm for Mont Ventoux, rather common values for ground ozone. Several of the Marshall Islands and Chesapeake Bay curves suggested the presence of ozone because of high attenuation below 3000 A, but it did not appear possible to derive significant ozone values.

Sulphur dioxide was identified several times from the spectra taken in Washington but never in Pasadena. The significant reason is probably that in the Washington area, coal is burned; whereas in the Pasadena area, oil and gas which have low sulphur content, are used exclusively. Glueckauf (9) reports that in the presence of ozone, air may be expected to be free of SO_2. On the night O_3 was present in Washington, SO_2 was absent; whereas, on December 13 and 18, 1950, SO_2 was present in a concentration of 0.08 ppm and the attenuation curves of Figure 2 did not have the shape or magnitude below 3100 A which would suggest ozone.

We have mentioned only a few of the many possible gaseous components of lower atmospheric air. The following are the nonvariable rare components according to a summary by Glueckauf: CO_2, A, Ne, He, Kr, Xe, H_2, CH_4, and N_2O. He also reports that the variable constituents of atmospheric air may include H_2O, O_3, SO_2, NO_2, CH_2O, I_2, NaCl, NH_3, and CO. Other workers include additional oxides of nitrogen. All of these constituents, both nonvariable and variable are generally present in low concentrations and only O_3, SO_2, and NO_2 produce detectable absorption in the spectral region and over path lengths with which we are concerned in this report. Water vapor absorption begins beyond our spectral limits. We were unable to identify positively absorption due to any of the gases except O_3 and SO_2, though the presence of NO_2 was suspected at Pasadena.

Tables of Spectral Attenuation

In all, some 80 σ vs. λ curves were obtained at Pasadena and 5 or more at each of the other locations. In so far as possible, the results for each place were combined into a family of curves covering the range of visibilities encountered. Tables 4, 5, and 6 of average spectral attenuation were prepared from the curves.

Pasadena – The selection of a single family of curves for Pasadena or the determination of a spectral attenuation formula depending on the single parameter, visibility, was necessarily based on a process of averaging. An empirical formula for the attenuation coefficient was derived by Baum (10) after study of all the data:

$$\sigma = 0.0036 \frac{(5380 - \lambda)}{V} + \left(\frac{800}{\lambda - 1800}\right)^3 \qquad (6)$$

where λ is in Angstroms and V in kilometers. This relation holds only for $4 < V < 40$ km and for $2400 < \lambda < 4000$ A. This formula was obtained from a series of plots of σ for some particular wavelength against σ_{5500A} or V. One point on each plot was determined from each spectrogram taken on the various nights. The points scattered widely, but the scatter was found to have a definite lower boundary; an envelope drawn along this boundary passed through or near the points associated with nights when the air was believed to be comparatively free of pollutants, such as just after a rain or during a mountain breeze. This envelope was taken to represent unpolluted or "clean air." For each ultraviolet wavelength studied, the envelope could be drawn as a straight line. These lines were found to have slopes and intercepts which could be related rather simply to wavelength resulting in Equation (6). Table 4 was prepared from this equation for wavelengths between 2400 and 4000 A and from the Linke-Borne formula with Middleton's (4) constants for wavelengths between 4000 and 6000 A. Curves drawn from each of these two independent formulae were found to join very well for visibilities extending from 4 to 40 km.

TABLE 4
Atmospheric Attenuation for Clean Air for Various Daylight Visual Ranges at Pasadena, California*

Wavelength (A)	Exponential Attenuation Coefficient (km^{-1})				
	3.9 km	6.5 km	7.8 km	13 km	39 km
	2.1 sm	3.6 sm	4.3 sm	7.1 sm	21 sm
2400	5.11	4.29	3.74	3.19	2.64
2600	3.56	2.79	2.28	1.77	1.25
2800	2.89	2.17	1.70	1.22	0.75
3000	2.49	1.80	1.39	0.96	0.51
3500	1.83	1.31	0.97	0.62	0.28
4000	1.32	0.94	0.68	0.43	0.18
4600	1.10	0.79	0.57	0.36	0.13
5000	1.05	0.75	0.54	0.33	0.12
5500	1.00	0.70	0.50	0.30	0.10
6000	0.96	0.66	0.47	0.28	0.09

*Conditions during measurements: path difference, 0.680 km; accuracy of individual measurements, ± 0.05 km^{-1} or less; dates of observations, March 1949 to April 1950 inclusive.

Chesapeake Bay and Dry Tortugas – The Chesapeake Bay data were analyzed in a manner similar to that described above. However, the scatter of points on the σ_λ vs σ_{5460A} plot was small and the points lay on a reasonably straight line; thus it was not necessary to consider a lower boundary as was done to obtain the coefficients for clean air for Pasadena. The Dry Tortugas data were similar and combined with the Chesapeake Bay data to yield Table 5 for $10 < V < 80$ km and $2970 < \lambda < 5780$ A.

Other Locations – Table 6 presents the attenuation coefficients obtained from the observations at the Marshall Islands for $15 < V < 80$ km and $3020 < \lambda < 5780$ A. The data taken on each of five nights in Nevada were so much alike that tables for a range of visibilities could not be prepared. In Washington, the number of nights studied was insufficient to warrant the preparation of a table.

TABLE 5
Atmospheric Attenuation for Various Daylight Visual Ranges at the Chesapeake Bay Annex and Dry Tortugas*

Wavelength (A)	Exponential Attenuation Coefficient (km^{-1})							
	9.8 km 5.3 sm	11.3 km 6.1 sm	13 km 7.1 sm	15.5 km 7.1 sm	19.5 km 11 sm	26 km 14 sm	39 km 21 sm	78 km 43 sm
2970	0.80**	0.73	0.66	0.58	0.51	0.44	0.37	0.30
3020	0.78**	0.70	0.63	0.55	0.48	0.41	0.33	0.26
3130	0.71**	0.64	0.57	0.50	0.43	0.36	0.29	0.22
3340	0.67**	0.60	0.54	0.47	0.40	0.34	0.27	0.20
3660	0.63**	0.56	0.50	0.43	0.36	0.30	0.23	0.16
4050	0.56**	0.50	0.44	0.38	0.31	0.25	0.19	0.13
4360	0.54**	0.48	0.42	0.35	0.29	0.22	0.16	0.10
5460	0.40**	0.35	0.30	0.25	0.20	0.15	0.10	0.05
5780	0.36**	0.32	0.27	0.23	0.18	0.14	0.09	0.05

*Conditions during measurements: path length, 2-1/2 miles over water; accuracy of individual measurements, ± 0.01 km^{-1}; dates of observation, CBA, February to April 1950 and Dry Tortugas, May 1950.

**Extrapolated from the data for $\sigma_{5460A} = 0.38$ km^{-1}

TABLE 6
Atmospheric Attenuation for Various Daylight Visual Ranges at the Marshall Islands*

Wavelength (A)	Exponential Attenuation Coefficient (km^{-1})				
	15.5 km 7.1 sm	19.5 km 11 sm	26 km 14 sm	39 km 21 sm	78 km 43 sm
3020	0.35**	0.31	0.28	0.24	0.20
3130	0.32**	0.28	0.24	0.21	0.17
3340	0.27**	0.24	0.21	0.18	0.15
3660	0.26**	0.23	0.19	0.16	0.12
4050	0.26**	0.21	0.17	0.13	0.09
4360	0.25**	0.21	0.17	0.12	0.08
5460	0.25**	0.20	0.15	0.10	0.05
5780	0.23**	0.18	0.14	0.09	0.05

*Conditions during measurements: path length, 4 miles over water; accuracy of individual measurements, ± 0.01 km^{-1}; dates of observations, March and April 1951.

**Extrapolated from $\sigma_{5460A} = 0.22$ km^{-1}

Extension of Tables to Fog and Other Cases of Atmospheric Murkiness

Tables 4, 5, and 6 do not give values of σ for V less than 4, 10, and 15 km, respectively. In the case of fog, where $V < 2$ km, Hulburt (11) has shown that σ is approximately independent of wavelength. Therefore one may extend the tables to shorter values of V, and obtain a rough idea of σ for all wavelengths for V less than these minimum visibilities given, by adding a constant c to the values of the second column of the appropriate table, where $c = 3.92/V - \sigma_z$ and where σ_z is the value at 5500 A in the second column of the appropriate table and V takes values from 0 to the minimum visibility given in the table. For

example, for V = 0.5 km in Pasadena, c = 6.8 and σ_{3000A}, σ_{3500A}, and σ_{4000A} are 9.3, 8.6, and 8.1 km^{-1}, respectively. These values compare favorably with the curve for November 22 in Plate B. However, this must be considered as an approximation only. Fogs were not investigated in the other geographical regions and we can only assume the above method might yield reasonable values of σ. Other cases of atmospheric murkiness such as rain, snow, sand storm, forest fire smoke, locust swarm, etc., will introduce complications not reflected in the tables.

Cautions in Selection and Use of Tables

It has been seen that the spectral attenuation curves generally appeared to follow particular patterns at each location. It is uncertain whether these patterns are typical of the haze for each locality and time of year, or whether they are accidental patterns for the haze prevailing during the time of the measurements. The tables are in effect the result of averaging over the varying degrees of atmospheric clearness for each of the patterns encountered. The tables have not received an extended test and should be used for guidance purposes only. However, they represent the only spectral attenuation data which are available for a variety of hazes having different σ vs. λ patterns and they also serve to illustrate the changes in the shape of the σ vs. λ curve which may arise at different localities when the visibility is the same.

Effect of Field of View – In applying the attenuation data presented in this report it must be borne in mind that they apply only to collimated light or where the receiver has very small (zero) field of view. As the field of view increases the effective attenuation decreases. This effect, for visible light, was discussed by Middleton (12), and has been studied by Stewart and Curcio (13). The latter used a distant point source, radiating over a hemisphere, and measured the radiation received as a function of the field of view of the receiver. They found that

$$T_\beta = T + g(1 - T) f(\beta) \qquad (7)$$

where T_β is the diffuse atmospheric transmittance measured with equipment having a field of view β radians in diameter, and T is the specular transmittance. The coefficient g depends on the reflectance of the terrain lying under the light path (in the case of a layer of low cloud lying above, this reflectance should also be included). The function $f(\beta)$ depends on the polar diagram of scattering. From experiments over water, for wavelengths 3600 to 6200 A, for V from 33 to 6.8 km and for β from 0.0524 to 0.436 radians (3 to 25 degrees), $gf(\beta)$ was found to be $0.5\,(1 - e^{-\beta})$. Then Equation (7) becomes

$$T_\beta = T + 0.5\,(1 - T)(1 - e^{-\beta}). \qquad (8)$$

If the reflectance of the terrain were unusually high, as for snow or a complete smooth cloud cover, g would be between 0.5 and 1, but g was not determined for these cases. To illustrate Equation (8), suppose that the receiver is at a distance from the point source in an atmosphere such that the specular transmittance, T, is 0.35. If the receiver has fields of view β = 0.262 radians (15°) and 0.524 radians (30°), from Equation (8) T_β has the values of 0.425 and 0.482, respectively, which are increases of 21 and 38 percent over T.

Effect of Ozone Below 3000 Angstroms – Because ground ozone concentration is so variable, it is not in general meaningful to show typical curves, formulae, or tables of spectral attenuation for $\lambda < 3000$ A. Below this wavelength, it is best to make direct measurements of attenuation. However, if the O_3 concentration is known from a chemical method, one can compute the absorption and add it to an empirical value of σ obtained from the

appropriate table for a given visibility. This is a stop gap procedure and we have not tested its reliability. In the case of the Pasadena data, from which Table 4 was prepared, values of σ for λ less than 3000 A were included, because these values were derived from actual measurements for over a year and serve to illustrate the situation as it was in Pasadena during the period March 1949 to April 1951.

CONCLUSIONS

The data which have been collected permit the following conclusions:

(a) Several different types of attenuation function are found in a city atmosphere unlike those found over the sea or in the desert; whereas, attenuation curves at stations outside cities appear to follow a particular pattern at each location.

(b) For similar visibilities the city data show a higher attenuation in the middle ultraviolet than do the data taken outside cities.

(c) The spectral attenuation curves for a Nevada desert are characterized by their proximity to Rayleigh scattering.

(d) It was difficult to determine the composition of smogs when they were encountered; but, under some conditions, it was possible to detect sulphur dioxide and to make approximate measurements of its concentration. Under clear weather conditions it was possible to detect ozone when it was present in the lower atmosphere and also to make approximate measurements of its concentration.

* * *

REFERENCES

1. Baum, W. A., and Dunkelman, L. (manuscript being prepared for publication)
2. Curcio, J. A., et al. (manuscript being prepared for publication)
3. Hulburt, E. O., J. Opt. Soc. Am., 31:467 (1941)
4. Middleton, W. E. K., "Visibility in Meteorology," 2nd Ed., Univ. of Toronto Press (1941)
5. Vassy, A., Doctorate Thesis, University of Paris (1941)
6. Collins, J. B., "A Haze Meter for Direct Measurement of Atmospheric Scattering Coefficient," Admiralty Research Laboratory Report ARL/R1/K904, March 1949
7. Pearson, C. A., Koomen, M. J., and Tousey, R., Bull. Am. Meteorol. Soc., 33:117 (1952)
8. Dessens, H., Ann. de Geophys, 2:276 and 343 (1946); 3:68 (1947)
9. Glueckauf, E., 'The Composition of Atmospheric Air' in "Compendium of Meteorology," American Meteorological Soc. (1951)
10. Baum, W. A., Doctorate Thesis, California Institute of Technology (1950)
11. Hulburt, E. O., J. Opt. Soc. Am., 25:125 (1935)
12. Middleton, W. E. K., J. Opt. Soc. Am., 39:576 (1949)
13. Stewart, H. S., and Curcio, J. A., J. Opt. Soc. Am., 41:876 (1951)

* * *

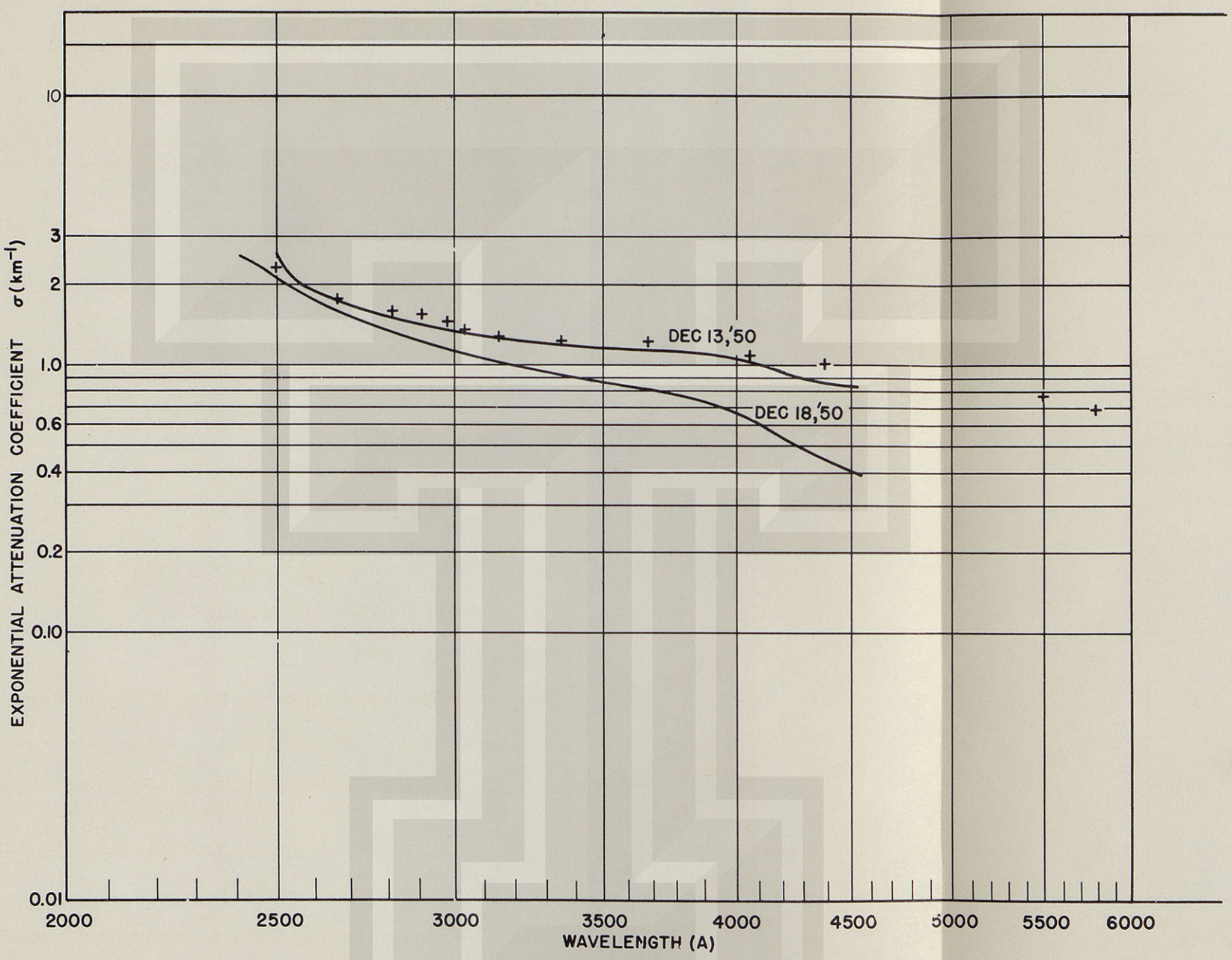

Figure 2 - Comparison between atmospheric attenuation coefficients obtained in Washington on December 13, 1950 using the continuous spectrum method (curve) and the line source method (points). A curve for December 18, 1950 also is shown. During these two nights the atmosphere was hazy and polluted with sulphur dioxide.

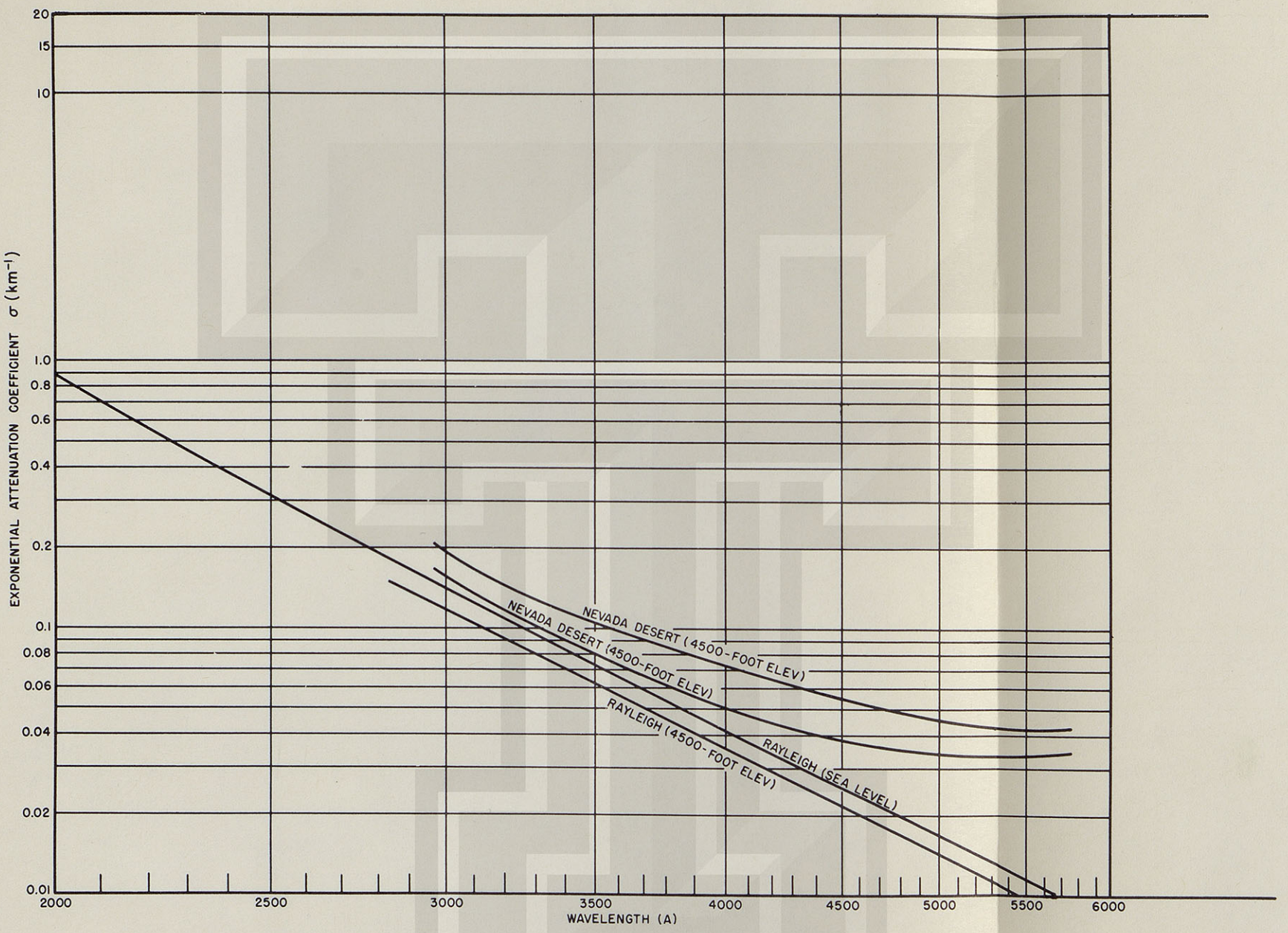

Figure 1 - Curves of horizontal atmospheric attenuation of ultraviolet and visible light in a Nevada desert at an elevation of 4500 feet; a Rayleigh scattering curve for this elevation is included for comparison.

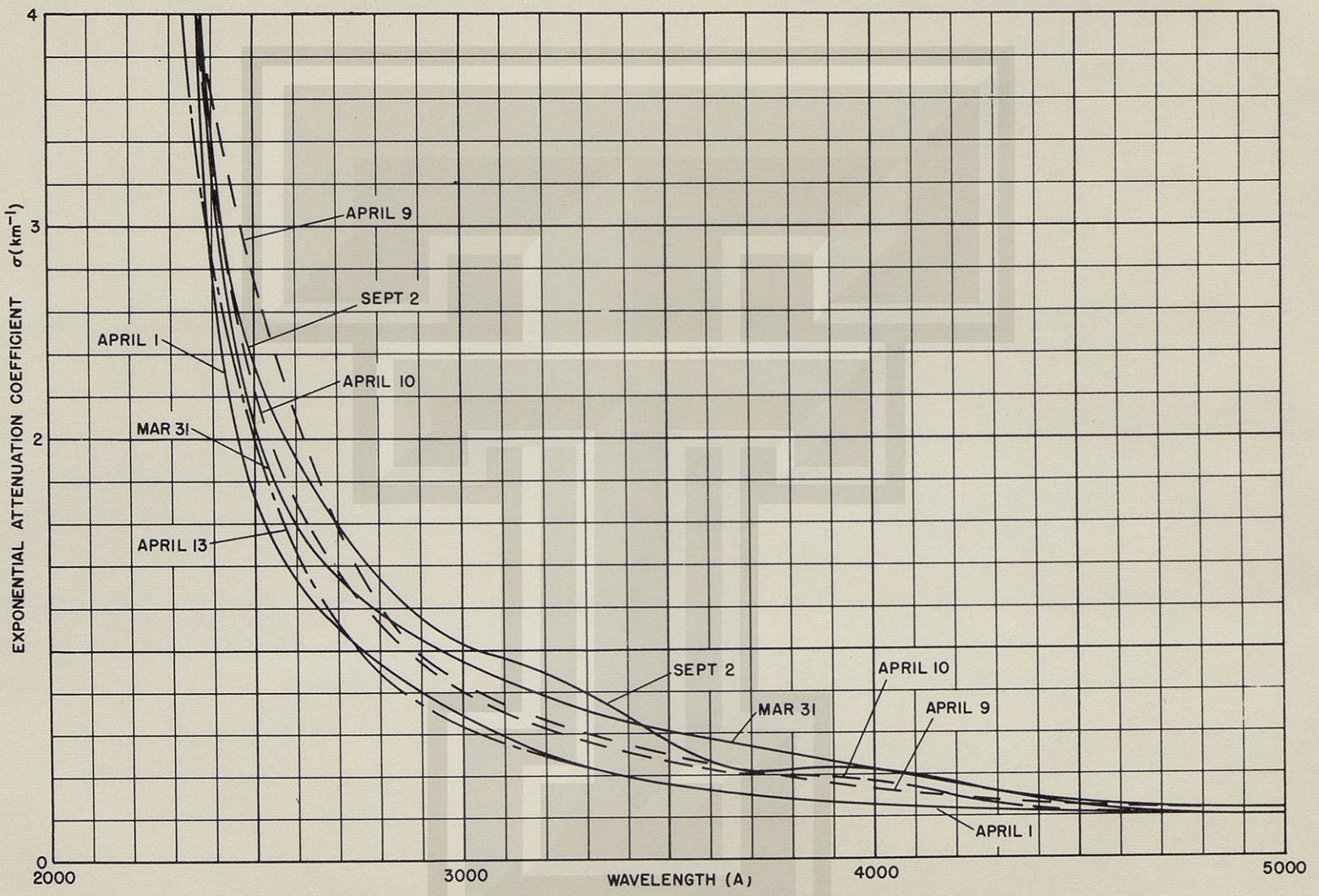

Figure 3 - Curves of horizontal atmospheric attenuation in Pasadena which illustrate how the curves may criss-cross and disagree in the ultraviolet for nights of approximately the same visual range

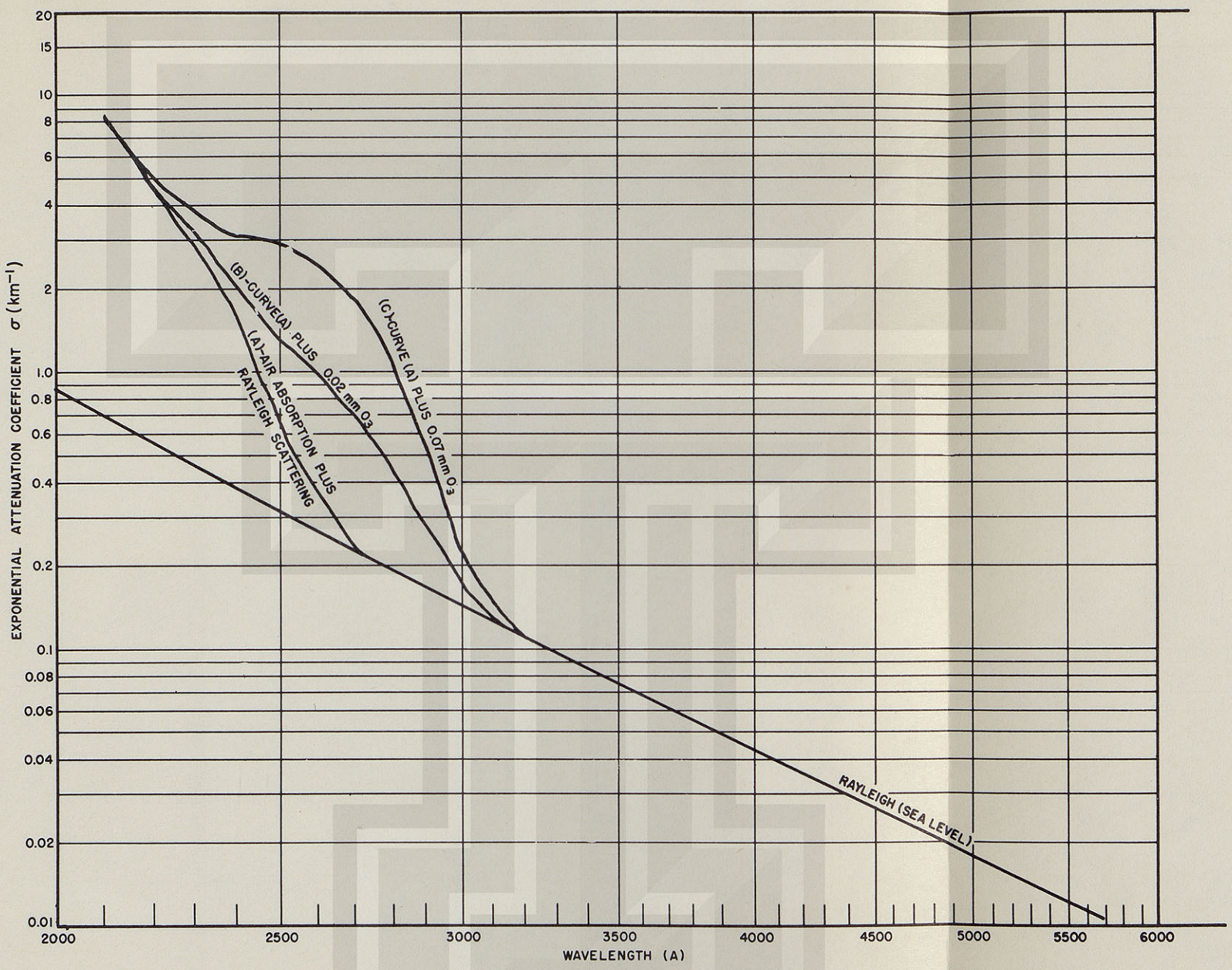

Figure 4 - Calculated curves of horizontal atmospheric attenuation of pure air (Rayleigh scattering plus absorption of air (Curve A)) and for air plus ozone in concentration of 0.02 parts per million (Curve B) and for air plus 0.07 parts ozone per million (Curve C)

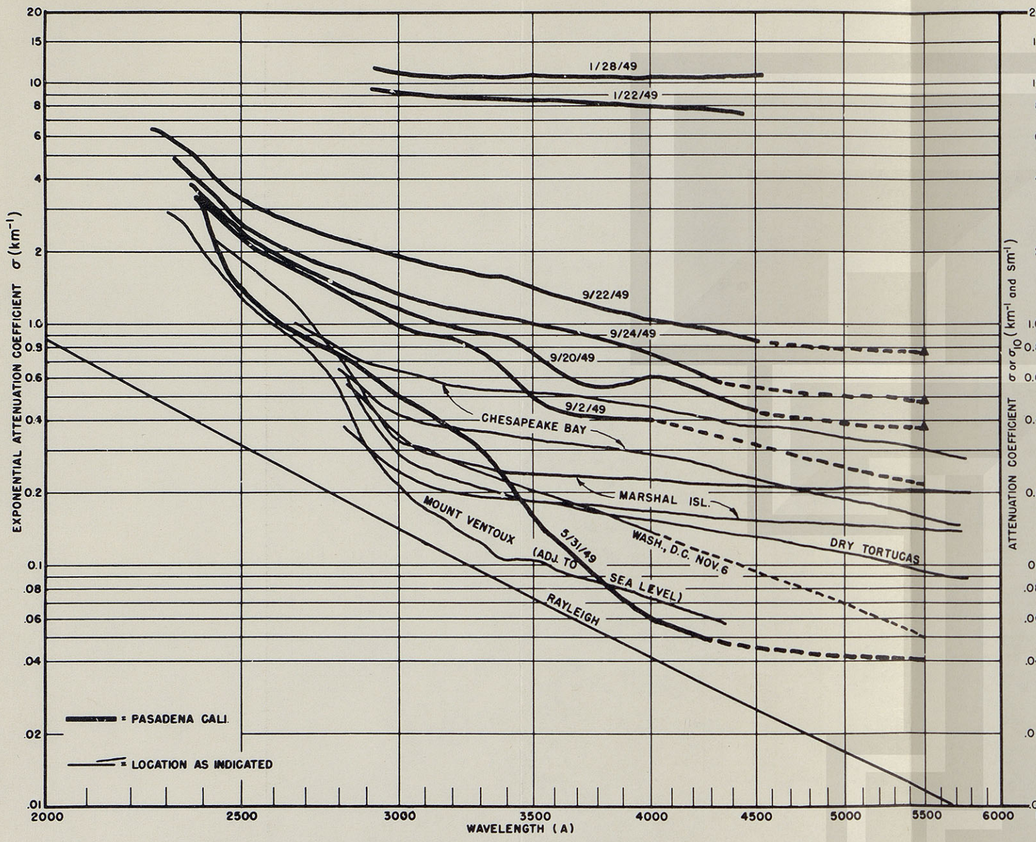

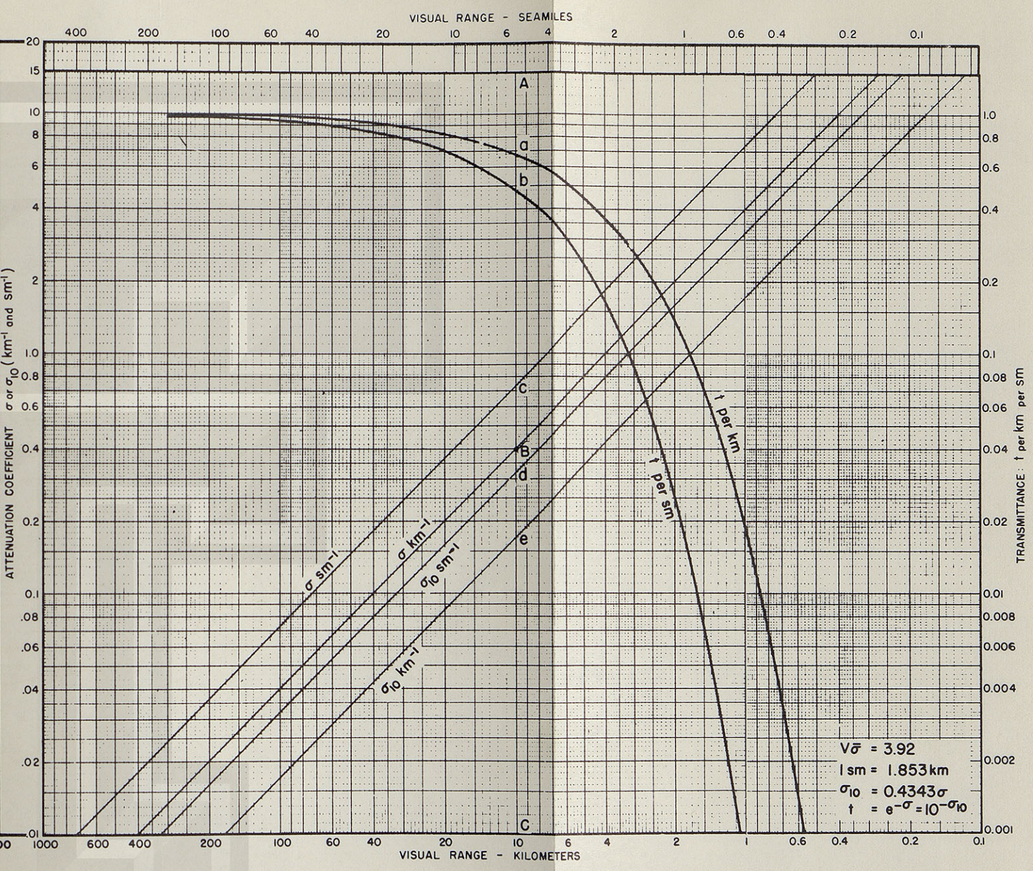

INSTRUCTIONS FOR USE OF CONVERSION DIAGRAM

In the diagram of Plate A, attenuation coefficients, $\sigma(km^{-1})$, $\sigma(sm^{-1})$, $\sigma_{10}(km^{-1})$ and $\sigma_{10}(sm^{-1})$ are plotted against visual range, V; these functions plot as straight parallel lines on log-log scales. Transmittance, t per km and t per sm are also plotted against V on log-log scales; these functions plot as curved lines. The σ scales are to the left and the t scales are to the right; σ and t take the units shown on the respective σ lines and t curves. V is given in km on the bottom scale and in sm on the top scale.

Conversion from any one of the coefficients; σ, σ_{10}, or t in either km or sm; to all others can be effected by moving along a vertical line through the value of the given coefficient on its appropriate curve. This vertical line intersects the σ lines and the t curves at points whose values are equivalent to the given value.

(The optical state of the atmosphere is characterized by the vertical line position which corresponds to the value for visual range. The visual range, however, has a true meaning only in dealing with 5500 A. But the visual range is also the path length through which the intensity of light of any wavelength is reduced to 1/50 of its original value. This distance may not always be of interest but nevertheless serves as the means for making desired conversions among σ, σ_{10}, and t for any wavelength.)

For example, to convert $\sigma(km^{-1}) = 0.39$ to the other terms and units, plot 0.39 on the $\sigma(km^{-1})$ line (see point B). Draw vertical line AC through B. Line AC intersects the t per km curve at point a, corresponding to t = 0.68 per km; AC intersects the t per sm curve at point b, corresponding to t = 0.49 per sm; the $\sigma(sm^{-1})$ line at c, $\sigma(sm^{-1}) = 0.72$; the $\sigma_{10}(sm^{-1})$ line at d, $\sigma_{10}(sm^{-1}) = 0.31$; and the $\sigma_{10}(km^{-1})$ line at e, $\sigma_{10}(km^{-1}) = 0.17$. V = 10 km = 5.4 sm.

Plate B - Typical curves of horizontal atmospheric attenuation of ultraviolet and visible light at Pasadena, California; Chesapeake Bay, Maryland; Dry Tortugas, Florida; Marshall Islands, Pacific Ocean; and Washington, D. C. Included for comparison are curves for theoretically pure air (Rayleigh scattering) and for exceptionally clean air obtained by A. Vassy at Mont Ventoux, Pyrennes.

Plate A - Diagram of conversion between attenuation coefficients, σ (base e) and σ_{10} (base 10), and transmittance, t. The length dimensions are in kilometers and sea miles.

F. VOLZ

ATMOSPHERIC TURBIDITY AND ITS SPECTRAL EXTINCTION

Reprinted from the Review
GEOFISICA PURA E APPLICATA - MILANO
Vol. 31, pp. 119-123 (1955)

ATMOSPHERIC TURBIDITY AND ITS SPECTRAL EXTINCTION

by F. Volz (*)

Summary — The indices of the wavelength dependency of the haze extinction which were currently determined from measurements of solar radiation and visibility at Mainz, show pronounced seasonal variations. The summer values are in genera definitely higher than in winter. There is no connection with the scatter light type of the sky-light or with the meteorological situation.

Zusammenfassung — Die Wellenlängenexponenten der Dunstextinktion, die in Mainz laufend aus Messungen der Sonnenstrahlung und der Sicht bestimmt wurden, zeigen starke jahreszeitliche Variationen. Insbesonders sind die Werte im Sommer meist deutlich höher als im Winter. Ein Zusammenhang mit den Streulichttypen des Himmelslichts oder der meteorologischen Situation besteht nicht.

Sommaire — L'exposant de la longueur d'onde de l'extinction brumeuse qui a été déterminé de façon continue des mesures de la radiation solaire et de la visibilité montre des fortes variations annuelles. Tout spécialement les valeurs sont d'été sensiblement plus élevées que celles en hiver. Une relation avec les types de lumière diffuse céleste et la situation météorologique n'existe pas.

For many problems of the atmospheric aerosol research it is desirable to know not only the total number of the nuclei, but also the size distribution and its variations. The different regions of the particle distribution are influenced in different manner by coagulation, sedimentation and exchange, in the clouds by precipitation and absorption of gases, and also by the production of aerosol by human activity and in nature. Especially for the optics of the atmospheric haze the size distribution in the radius range between $r = 0.1$ and $1\,\mu$ is very important. While the direct measurements by Junge with nuclei- and ioncounter and impactor nearly every day in the high mountains and in the lowlands show a distribution following the law $dN/d\log r \sim r^{-3}$ $(0.05 < r < 20\,\mu)$, the analysis of the *sky-light* often shows greater deviations from a power law (2).

Also from the measurement of the dependence of the *haze extinction* on the wavelength, one can receive data concerning the size distribution. New results may be briefly reported. The Fig. 1 shows schematically how the complex haze extinction is obtained by summarizing the extinction coefficients (*Mie*-efficiency functions) of all particle groups. If the frequency of the particles obeys the law r^{-3} (upper right), the extinction follows the *Ångström* law $a \sim \lambda^{-\alpha}$ with $\alpha = 1$

(*) Dr. F. Volz, Meteorologisch-Geophysikalisches Institut der Johannes Gutenberg Universität, *Mainz*.

from $\lambda = 0.2$ to $10\,\mu$. From Fig. 1 we may also see that large particles affect the extinction only at large wavelenghts, very small particles at short wevelengths. Dashed curves are for double frequency, dotted curves for half frequency of parti-

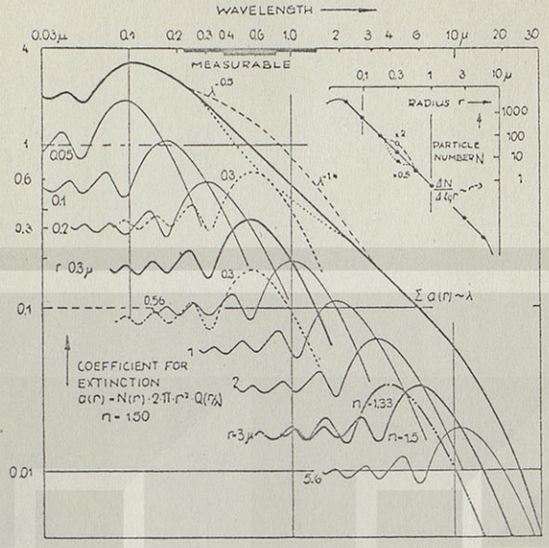

Fig. 1 - *The sum of the* MIE *efficiency functions of different particle groups gives the spectral haze extinction.*

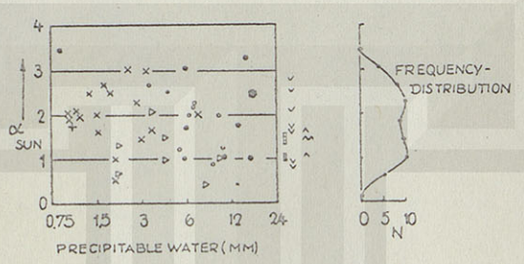

Fig. 2 - *Single values of the wavelength exponent* α *and the frequency distribution of the haze extinction from Smithsonian measurements, after* GOETZ (sign o, unpublished), SCHUEPP ([3]) (∧ ∨ o) *and* VOLZ (Mount Wilson ⊙, Montezuma X Δ).

cles with $0.3\,\mu$ radius. Such a particle distribution occurs with the sky-light type *C* resp. *A*. It is easy to see that the λ-dependency of the extinction is sensitive to small deviations from the power law. Finally it can be noticed that the measurement of radiation in the visible part of the spectrum can only give information on the size distribution of the nuclei with radii between 0.1 and $1\,\mu$.

If the size distribution follows a generalized law $dN/d\log r \sim r^{-v}$, than we get theoretically the law $a_\lambda \sim \lambda^{-\alpha}$, where $\alpha = v - 2$. ÅNGSTRÖM and others found a mean $\alpha = 1.3$, but one has often found α-values between 0.5 and 2. Fig. 2 shows single α-values taken from the Smithsonian measurements of the solar radiation on high mountains.

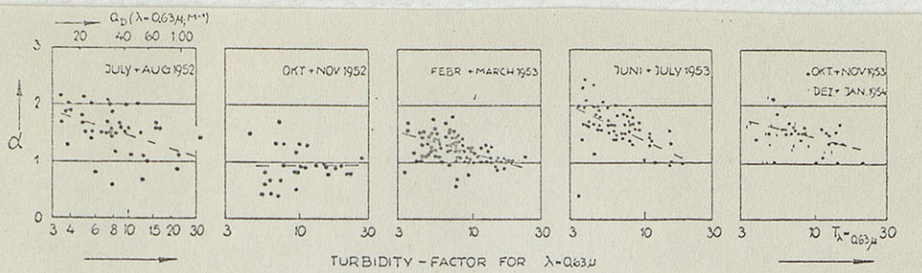

Fig. 3 - *The values of α_{sun} at Mainz show an annual variation.*

In Mainz we have made continuous measurements of the solar radiation with a spectral photometer (2). A selenium cell and Schottfilters with $\lambda_{eff} = 0.38$ to

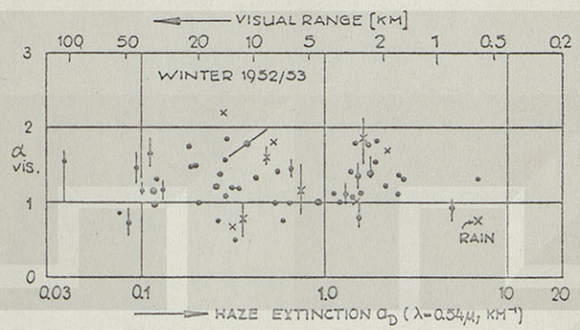

Fig. 4 - *α-values from horizontal attenuation at Mainz in winter.*
X October to December 1952, Frankfurt, 10 days;
• January to March 1953, Frankfurt and Mainz, 27 days.

0.76 μ are used. Also measurements of the horizontal extinction have been made in blue and red with the visibility-photometer by LOEHLE, if the sky was cloudless. Then we have calculated the α-values of the haze extinction. The α_{sun}-and α_{vis}-values have an accuracy of about 5 %, but visibility measurements at the same time of different objects (dark forests and roofs) often give greater differences. This may be caused by unequal haze density, partially by industrial smoke.

Fig. 3 shows the α_{sun}-values of the turbidity above Mainz, characterizing the haze in the ground layer, in dependence on the turbidity factor, and separated for different parts of the year. Each day is marked by one sign only, if α does not change in a remarkable way. The α-values are in summer mostly higher than in winter and increase in summer often with decreasing turbidity. It seems that α_{sun} has a noticeable annual variation, the measurements by WEMPE (4) indicate a similar variation.

Now, what about the measurements of *visibility*, which characterizes the haze near the earth's surface? According to Fig. 4 the values of α_{vis} reveal in winter the same value within all occuring visibility-ranges. During summer the level is remarkably higher. — The trend of different shorter series of daytime and nighttime measurements of α_{vis} (5) is shown in Fig. 5. The mean level is considerably